

QATAR UNIVERSITY

COLLEGE OF ARTS AND SCIENCES

ENHANCEMENT OF THE INTERFACIAL ADHESIVE STRENGTH BETWEEN LOW
DENSITY POLYETHYLENE AND ALUMINUM FOIL FOR PACKAGING
APPLICATIONS

BY

TAGHREED ABDULHAMEED AL-GUNAID

A Thesis Submitted to
the College of Arts and Sciences
in Partial Fulfillment of the Requirements for the Degree of
Master of Science in Material Science and Technology

June 2021

© 2021 Taghreed. All Rights Reserved.

COMMITTEE PAGE

The members of the Committee approve the Thesis of
Taghreed Al-Gunaid defended on 27/04/2021.

Dr. Igor Krupa
Thesis/Dissertation Supervisor

Dr. Khaled Youssef
Committee Member

Dr. Anton Popelka
Committee Member

Approved:

Ibrahim AlKaabi, Dean, College of Arts and Sciences

ABSTRACT

AL-GUNAID, TAGHREED A., Masters: 2021, Material Science and Technology

Title: ENHANCEMENT OF THE INTERFACIAL ADHESIVE STRENGTH BETWEEN LOW DENSITY POLYETHYLENE AND ALUMINUM FOIL FOR PACKAGING APPLICATIONS

Supervisor of Thesis: Dr. Igor Krupa

The low-density polyethylene/aluminum (LDPE/Al) joint in Tetra Pak[®] liquid containers provides stability and strength to the food package, ensures protection against outside moisture, and maintains the nutritional values and flavors of food without needed for additives in the food products. However, the poor adhesion of LDPE to Al, due to the inert non-polar LDPE surface, is a limiting factor and extra polymeric interlayers or surface treatment is required. Two surface modification techniques were employed in order to identify the most appropriate method that achieves stronger adhesion properties, which are : air-flow corona discharge, and corona plasma assisted grafting of the LDPE surface with different molecular weight compounds of polyethylene glycol (PEG) .In brief, it was found that these surface modification techniques contributed to significantly improvement in wettability and polarity of the LDPE surfaces as was confirmed by contact angle measurements. The chemical composition changes after plasma treatment and PEG grafting-to processes were observed by X-ray photoelectron spectroscopy (XPS) and Fourier transform infrared spectroscopy (FTIR). Furthermore, surface roughness and morphology were analyzed before and after LDPE surface treatment by scanning electron microscopy (SEM) and atomic force microscopy (AFM). Adhesion characteristics of LDPE/Al adhesive joints

were analyzed by the mechanical peeling test as well as thermodynamic work of adhesion. The most significant adhesion improvement of the LDPE /Al laminate was achieved for corona-treated 10.0 wt.% PEG (6000M) based-aqueous solution grafted into LDPE surface, where the peel resistance value was 163 N/m.

DEDICATION

A special feeling of gratitude and thankful to my ideal parents, Abdulhameed & Rahma. They have been, and continue to be, a source of endless love, encouragement, and inspiration throughout all my life. Without them, none of my success would be possible.

ACKNOWLEDGMENTS

First and foremost, all the praises and thanks to Allah SWT, for his showing all the countless blessings during my masters, and for giving me the strength and persistence, the patience and endurance, and the great opportunities to complete this thesis successfully and completely satisfied.

There are a number of people and supporters whom I am very grateful and appreciative for what they have done for me during my academic studies. Without a doubt, I would not have written this thesis without their persistent help and encouragement. I will mention them as follows:

I would like to express my profound gratitude and most sincere appreciation to my thesis supervisor Dr. Igor Krupa, who offered a great opportunity to do my master thesis under his guidance and for his encouragement in carrying out this work. Furthermore, I am extremely grateful and thankful to Dr. Anton Popelka for all the instructions and assistance he gave them to me. His patience, vision, sincerity, and motivation have deeply inspired me. It was great privilege and honor to work under his direction.

I am thankful for the all faculty members of the Material sciences and Technology Program, Dr. Talal M. Al-Tahtamouni, Dr. Khaled M. Youssef, Dr. Ahmed Elzatahry ,Dr. Mohamed K. Hassan, and Dr. Abou bakr M. Ali for their valuable effort, time and support since I was joined this academic program.

Moreover, I want to extend my profound acknowledgement for Qatar Petrochemical Company (QAPCO) for providing the financial support to this project [grant QUEX-CAM-QAPCO-20/21]. I very much appreciate your support and cooperation. Special thanks to Dr. Mabrouk Ouederni , the manager of the product development & innovation

section at QAPCO and Dr. Senthil Kumar Krishnamoorthy , a lead Engineer at QAPCO.

I would like to thank Dr.Peter Kasak , Dr.Patrick Sobolciak , and Dr.Fathima Sifani Zavahir for their precious knowledge, instruction, and suggestion, .The assistance provided by them is greatly appreciated. Furthermore, I will forever be grateful and appreciative to Eng.Asma Abdulkareem for providing help and support to me.

I acknowledge the efforts of all the lab technicians, whom I met during my research work at Qatar University, at the Center for Advanced Materials (CAM), Gas Processing Center (GPC), and Central Laboratory Unit (CLU). They had actively and effectively contributed for conducting the required characterization tests for my samples. All thanks, appreciation, and respect for their efforts.

Last but not least, I am wholeheartedly grateful to my family for having always believed in me and for their continued encouragement to achieve my dreams. My friends, work colleagues, and all the people I have met during my master's journey deserve special mention for their love, faith, and support. Without their encouragement and kindness, this project could not have been completed.

TABLE OF CONTENTS

DEDICATION	v
ACKNOWLEDGMENTS	vi
LIST OF TABLES	x
LIST OF FIGURES	xi
Chapter 1: INTRODUCTION.....	1
1.1 A brief study of polyethylene (PE)	1
1.1.1 General background.....	1
1.1.2 Classification of polyethylene (PE).....	2
1.1.3 PE in food packaging applications (Tetra Pak container)	3
1.1.4 Surface characteristics of PE	5
1.2 Surface modification techniques of polyethylene	6
1.3 Polymer-metal adhesion.....	9
1.4 Problem statement.....	12
1.5 Research objectives	12
Chapter 2: LITERATURE SURVEY	13
2.1 Surface modification techniques of hydrophobic polymers.....	13
2.1.1 Corona discharge	13
2.1.2 Chemical modification via grafting with PEG monomers	16
Chapter 3: METHODOLOGY	20

3.1 Materials.....	20
3.2 Experimental apparatus/equipment.....	22
3.3 Experimental procedure	23
3.3.1 Preparation of LDPE thin sheets and LDPE-Al laminate.....	23
3.3.2 Pre-treatment of LDPE sheets	25
3.3.3 Surface modification of LDPE surface using corona discharge.....	25
3.3.4 Grafting of PEG/PEO onto LDPE surfaces beside corona discharges	26
3.3.5 Grafting efficiency (%GE) calculation.....	27
3.3.6 Determination of surface wettability	27
3.3.7 Determination the adhesion strength of LDPE/Al laminate.....	28
3.3.8 Calculation of the work of adhesion.....	30
3.4 Characterization and analytical techniques	31
3.4.1 Investigation of the thermal properties	31
3.4.2 Surface morphology analysis.....	32
3.4.3 Surface composition evaluation.....	33
Chapter 4: RESULTS AND DISCUSSION	35
4.1 Thermal analysis of LDPE	35
4.2 Surface modification by corona discharge	38
4.2.1 Surface wettability analysis	38
4.2.2 Surface morphology analysis.....	41

4.2.3 Surface compositions evaluation	43
4.2.4 Adhesive strength measurements	47
4.3 Chemical modification of LDPE surfaces by free radical grafting with polyethylene glycol derivatives (PEG/PEO) in combination with corona discharge	49
4.3.1 Grafting efficiency (% GE) calculation	49
4.3.2 Surface wettability analysis	50
4.3.3 Surface morphology analysis.....	55
4.3.4 Chemical composition investigation	60
4.3.5 Adhesive strength measurements	64
Chapter 4: CONCLUSION	67
Chapter 5: FUTURE WORK	68
REFERENCES	69

LIST OF TABLES

Table 1 The physical properties and potential uses of the tested LDPE grades	20
Table 2 List of used equipment.....	22
Table 3 Surface free energy and its components of the testing liquids at 23 °C	28
Table 4 Melting and crystallization parameters for LDPE grades according to DSC measurements.....	36
Table 5 Elemental composition of untreated and corona-treated LDPE grades from XPS	

observations	47
Table 6 elemental composition of LDPE surfaces by XPS analysis	63

LIST OF FIGURES

Figure 1 The chain microstructures of PE classifications.....	3
Figure 2 Synthetic plastics used in the packaging industry worldwide (in percent) in 2015.....	4
Figure 3 Components of Tetra Pak inside packaging layers.....	5
Figure 4 Surface activation reactions by plasma radiation	8
Figure 5 General classification of grafting mechanism	9
Figure 6 Mechanism of mechanical interlocking.....	10
Figure 7 Schematic of dynamic contact angle at solid-liquid-gas contact line.....	11
Figure 8 Corona discharge configuration	14
Figure 9 Chemical structure of PEG and PEO polymers.....	17
Figure 10 LDPE thin sheet preparation	24
Figure 11 Solid-state pure polyethylene glycols.....	27
Figure 12 Scheme of proposed grafting mechanism of PEG/PEO onto corona-treated LDPE.....	27
Figure 13 90° peeling test on LDPE/Al adhesive joint.....	29
Figure 14 Illustrative scheme of work of adhesion between LDPE substrate and Al film	31
Figure 15 DSC-8500, PerkinElmer® instrument.....	32
Figure 16 Fourier-transform infrared spectrometer (FTIR).....	34
Figure 17 X-ray Photoelectron Spectroscopy (XPS), Kratos Axis Ultra DLD instrument	

.....	34
Figure 18 DSC (A) melting and (B) crystallization curves of LDPE specimens	37
Figure 19 Contact angle ($^{\circ}$) of LDPE samples vs. corona-treatment time (sec.).....	40
Figure 20 Surface free energy and its components (mN/m) of LDPE samples vs. corona-treatment time (sec.).....	41
Figure 21 SEM images of LDPE Competitor surfaces : (A) untreated , (B) corona - treated (t=5s).....	42
Figure 22 SEM images of LDPE EC01-041 surfaces : (A) untreated, (B) corona - treated (t=5s).....	42
Figure 23 SEM images of LDPE EC01-049 surfaces : (A) untreated, (B) corona - treated (t=5s).....	43
Figure 24 SEM images of LDPE EC02 surfaces: (A) untreated, (B) corona - treated (t=5s).....	43
Figure 25 FTIR spectra of untreated and surface-treated LDPE grades.....	45
Figure 26 XPS spectra of LDPE grades : untreated (1) and 1 sec. corona-treated (2)	46
Figure 27 peel resistance,work of adhesion of LDPE/Al laminates as a function of corona treatment time of LDPE surfaces	48
Figure 28 influence of surface treatment by corona discharge on GE (%) of PEG/PEO-g-LDPE surfaces	50
Figure 29 Contact angle of untreated and plasma -treated	52
Figure 30 Contact angle of untreated and plasma -treated	53
Figure 31 Contact angle of untreated and plasma -treated	53
Figure 32 Surface energy (γ_s) and its derivatives: polarity (γ_{sp}), and dispersion (γ_{sd}) of untreated and corona treated.....	54

Figure 33 SEM micrographs of PEG-g-LDPE (1,000M) water solution	56
Figure 34 SEM micrographs of PEG-g-LDPE (6,000M) water solution	57
Figure 35 SEM micrographs of PEO-g-LDPE (300,000M) water solution	57
Figure 36 AFM images with Ra roughness parameter of (a) untreated (b) corona treated LDPE surfaces	59
Figure 37 AFM morphological images and line scans of corona activated LDPE films which surface grafted by PEG (1000M) aq. solutions with concentration of (a) 1.5 wt.% , (b) 10.0 wt.%.....	59
Figure 38 AFM morphological images and line scans of corona activated LDPE films which surface grafted by PEG (6000M) aq. solutions with concentration of (a) 1.5 wt.% , (b) 10.0 wt.%.....	59
Figure 39 AFM morphological images and line scans of corona activated LDPE films which surface grafted by PEO (300,000M) aq. solutions with concentration of (a) 1.5 wt.% , (b) 5.0 wt.%	60
Figure 40 FTIR spectra of LDPE surfaces:.....	62
Figure 41 XPS spectra of LDPE surfaces	63
Figure 42 Effect of corona treatment on the peel resistance and work of adhesion of PEG/PEO-g-LDPE adhesive joint with Al.	66

CHAPTER 1: INTRODUCTION

1.1 A brief study of polyethylene (PE)

1.1.1 General background

Polyethylene (PE) is the most common polyolefin that is found in large scale in the commercial markets as well as is considered among the top five world's largest productions and consumptions of synthetic resin [1-3]. Polyolefins are thermoplastic polymers (thermo-softening plastics). They are flexible and moldable upon heating, and solid and rigid upon cooling [4]. Polyethylene (PE) is derived from petrochemical sources such as crude oil and natural gas by catalytic polymerization of low molecular weight ethylene (C_2H_4). [5], whereas it is formed by the chemical connection of thousands of repeated units of ethylene (C_2H_4) monomers in the presence of a catalyst that contributes to break the double bond in ethylene and thus connect carbon atoms in the polymeric chain [3].

Polyethylene (PE) subdivided into several types/grades according to respective polymerization process, PE density and degree of chain branching. The three most common PE grades are: high density polyethylene (HDPE), low density polyethylene (LDPE), and linear low density polyethylene (LLDPE) [6].

To prepare HDPE, Ziegler-Natta polymerization was carried out under medium-pressure (15-30 atm) in the presence of organic compound catalytic. Under these conditions, the polymerized PE molecules were linear and the molecular chain was very long with a molecular weight up to several hundred thousand. If produced under high-pressure (100-300 MPa), high temperature (190-210 °C) and in peroxide catalytic conditions free radical polymerization, the end product would be low-density polyethylene (LDPE) which was a branched structure.[7]

1.1.2 Classification of polyethylene (PE)

As already mentioned above, polyethylene (PE) is divided into three main types, which are: LDPE, LLDPE, and HDPE [8, 9]

- Low-density polyethylene (LDPE):

LDPE is a solid with a slightly transparent color with density range is 0.915–0.930 g/cm³, so it has the lowest value of density in the comparison with other types of PE. It is able to withstand temperatures up to 80 °C constantly and 95 °C for a short time. The crystallinity of LDPE usually varies between 50 and 70%. In addition, LDPE has excellent chemical resistance against many chemical compounds, especially acids, alkalis, and inorganic solutions. In contrast, it is susceptible to hydrocarbons, halogenated hydrocarbons, oils and greases, since these compounds cause swelling (increasing the original thickness). Furthermore, essential oils and vegetable oils cause the environmental stress cracking (ESC) of LDPE, and this effect can be minimized by using of higher molecular weight grades of LDPE. ESC means the appearance of cracks on the surface of a material or completion of its failure and thus leads to multi-axial stress in case it comes into contact with certain liquids or vapors. Lastly, LDPE is the largest single polymer that is used in food packaging in both film and blow-molded forms.

- Linear low-density polyethylene (LLDPE):

LLDPE density lies between 0.915 and 0.940 g/cm³. Its structure consists of a linear sequence of carbon atoms bonded to hydrogen atoms with many short branches. It is usually synthesized by polymerization of ethylene with long chain olefins. LLDPE is remarkable by high tensile strength and impact and puncture resistance than LDPE, but it has narrower molecular weight distribution compared to LDPE. Moreover, LLDPE is extremely flexible and has the capacity to elongate under the influence of tension, as

well as it has good electrical conductivity and properties. LLDPE is involved mainly in the Packaging purposes.

- High-density polyethylene (HDPE):

It is known for its large strength-to-density ratio, where its density lies between 0.940 to 0.970 g/cm³. Thus, it has the highest density compared to the rest of PE. HDPE has higher intermolecular strength and tensile strength in compare with LDPE. In fact, HDPE has Short chain branching at the polymer backbone than LDPE and thus exhibits a higher crystallinity (up to 90%). HDPE is used in several industrial applications, mainly preservation packages and bottles (for food products, detergents, and cosmetics), fuel tanks, pipelines and housewares.

The difference in the chain branching of PE types is shown in Figure 1.

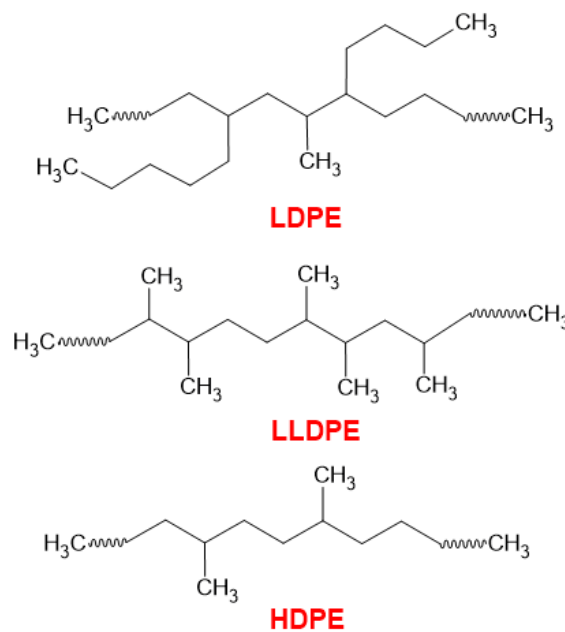


Figure 1 The chain microstructures of PE classifications

1.1.3 PE in food packaging applications (Tetra Pak container)

Polyethylene (PE) is the most common polyolefin that is used in large scale in the food processing and packaging applications, where LDPE (low-density polyethylene) and LLDPE (Linear low-density polyethylene) were ranked the first in the food packaging

industry in recent decades [1]. The increased trend to involve the polyolefin materials including low density polyethylene (LDPE) and high density polyethylene (HDPE) in the food packaging industry due to their unique physical and chemical characteristics, light weight, non-corrosive, durable , easy to use and re-shape , cost effectiveness, and have good barrier against moisture and water vapor in compare with conventional materials [2, 10-13]

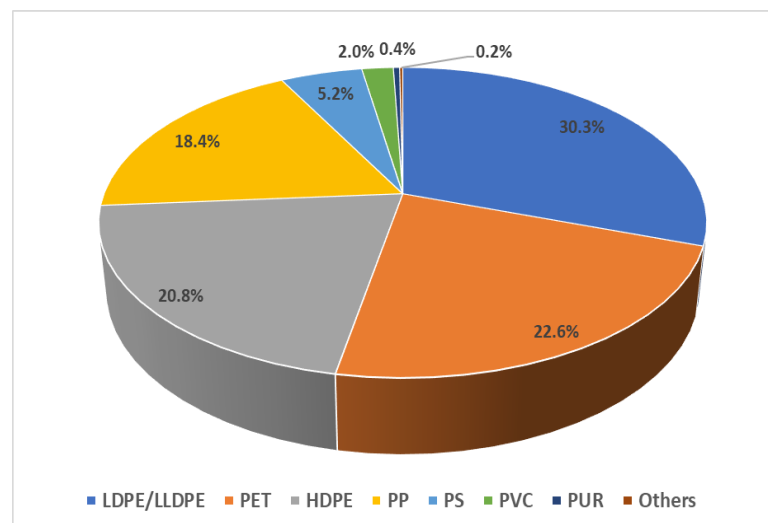


Figure 2 Synthetic plastics used in the packaging industry worldwide (in percent) in 2015 [1]

Tetra Pak® is a Swedish-Swiss multinational company that specializes in the food packaging containers to almost all countries. It was established in 1951 in Lund, Sweden by Dr. Ruben Rausing and Erik Wallenberg, the founders of Tetra Pak [14]. In the 21th Century it becomes the world-leading company in manufacturing the most sustainable food packaging products. The structure of Tetra Pak containers have aseptic packaging, which means their inner packaging is primarily made of six-layers paperboard (75%), polyethylene (20%), and aluminum (5%) that are combined in specific order under the influence of heat and pressure, as shown in Figure 3 [15-17]. Paperboard is used in order to provide stability and strength to the container, while polyethylene protects the interior cover against outside moisture, and aluminum foil is

effective in protecting the inner packaging against oxygen and light , which leads to maintain the nutritional value and flavors of the food in the package [18, 19].

Tetra Pak containers are distinguished by [15]:

- Lightweight and easy to transport since they are made mostly of thin layers of paperboard.
- Eco-friendly and fully recyclable because paperboard is a renewable raw material, Al is a metal that is 100 percent recyclable, and PE can be recycled using special plastic recycling processes.
- Optimum shelf life which leads to extend the life of the liquid product by several months.
- Excellent storage of various fluids with a long expiration date without need for additives into the food products.

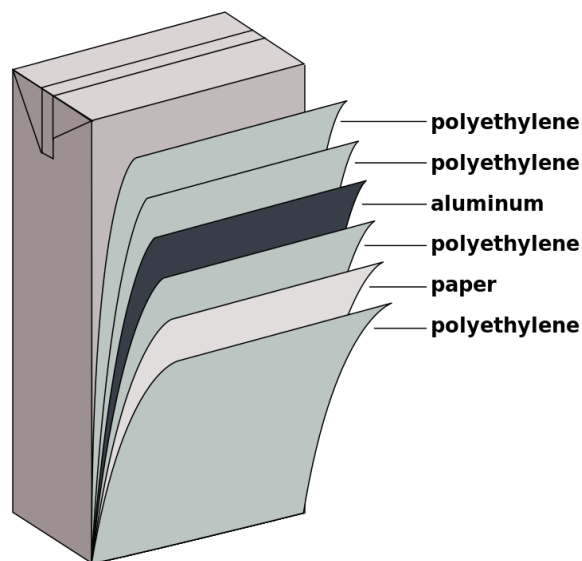


Figure 3 Components of Tetra Pak inside packaging layers [20]

1.1.4 Surface characteristics of PE

PE materials is characterized by their weak surface properties , including adhesion, wettability, and cytocompatibility, that impede their integration with other metals to form multi-layered laminates which are used later in food packaging applications [21].

In fact, PE materials have inert (low surface reactivity) and hydrophobic (poor wettability) nature due to the lack of functional groups and low proportion of polar regions on their surfaces, and therefore incomplete adhesion with other materials [21, 22]. So it is necessary to modify the surface characteristics of PE before lamination using the appropriate surface modification technique.

1.2 Surface modification techniques of polyethylene

Polymer surface modification has been the subject of a large number of investigations by academic and industrial sectors, but it has not been sufficiently shed light on the potential techniques for polymer surface activation which can contribute to make certain polymer-based surfaces receive value-added interfaces such as inks, coatings, and adhesive formulations [23].

Several surface modification techniques are employed in enhancement PE surface characteristics to raise their surface energy, resulting in better wettability and thus higher bond strength with other metals [10]. The surface modification methods are basically classified into three sections: physical modification based on plasma technologies and flame treatment, chemical modification *via* surface functionalization, and mechanical abrasion [3, 11, 24]. However, previous studies have found that mechanical methods based on abrasion has limited effectiveness as well as could cause large damage of the treated surfaces [25, 26]. The flame treatment is difficult to control, and bonding must be carried out shortly after exposure to flame [10]. Therefore, it is preferable to use either physical methods based on plasma techniques or chemical methods in the surface treatment of polyolefin.

Plasma technologies are considered the efficient method for surface treatment of the polymeric surfaces without affecting on their bulk properties [27]. Plasma is known as the fourth state of matter after solid, liquid, and gas. It represents as highly ionized gas

contains opposite-charged particles atoms and electrons, as well as neutral species and it created by high energy of radiation or electric field [28, 29]. Plasma technologies are categorized based on various parameters such as electronic density, pressure, and temperature [30]. The commonly used plasma technologies in industrial applications are hot or thermal plasmas ,which performs in near equilibrium particular condition , and cold or non-thermal plasmas , which operates in a non-equilibrium state under most operating conditions [31].

Hot plasmas include electric arcs, plasma jets of rocket engines, and thermonuclear reaction generated plasmas. On the other hand, cold plasmas include corona discharge, low-pressure direct current (DC) and radio-frequency (RF) discharges [30]. Hot plasmas are known for high temperature of both charged and neutral reactive particles and the high-energy electrons. The supply gas is heated to a high temperature (usually in the range of 20000 K) to achieve the greatest amount of gas ionization, and therefore it can be asserted that the degree of ionization in the hot plasma is much higher compared to the cold plasma, as it sometimes reaches the maximum degree (100%) [32].

In contrast, cold plasma consists of two types of particles: high-temperature electrons 1-10 electron-volt (eV)¹ and heavy particles (i.e., neutral or charged particles) that have low temperatures close to room temperature but less than the electron temperature [31]. Cold plasma is created when an electrical power source is applied to the supply gas, which cause to its ionization, then multiple reactive species are formed [33]. However, cold plasma is characterized with low degrees of ionization between 10^{-4} and 10% at maximum [34].

¹ Electron temperature in the cold plasma flow lies between 1 eV = 11604.52 kelvin and 10 eV = 116045.25 kelvin

The surface treatment of polymer surfaces by cold plasma is based on the ionization of the feed gas and dissociation into electrons, radicals, natural particles, and reactive particles containing nitrogen, oxygen or hydrogen terminals and at low temperature. These ions and particles (plasma flow) accelerate into the polymer surfaces, where the interaction between the surface atoms and plasma flow can be formed into several surface activation reactions such as functionalization, deposition, etching, or cross-linking [35, 36].

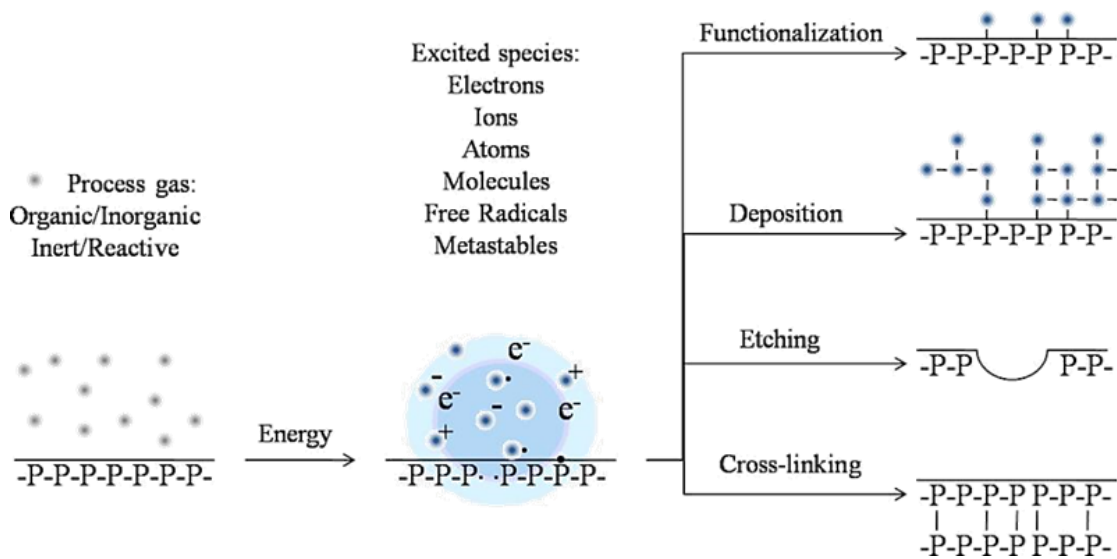


Figure 4 Surface activation reactions by plasma radiation [36]

In addition, chemical modification of the polymeric surfaces with techniques based on grafting play vital role in the biomedical, environmental, and industrial applications [37, 38]. These surface modification techniques contribute to positive changes in the physical and chemical properties, morphology, and biocompatibility of the polymer [39-41] due to impart a variety of functional groups on its surface [42, 43]. There are many different approaches of synthetic grafting, such as atom transfer radical polymerization (ATRP), ring-opening metathesis polymerization (ROMP), anionic and cationic polymerizations, and free radical living polymerization [44]. Free radical graft copolymerization is common chemical method for modifying the properties of

polymers, where initiators/monomers are used to initiate the free radicals in the chemical grafting process, which results in the transfer of the high-energy radicals to the substrate polymer thus monomers are covalently attached to specific regions within the backbone of the parent polymer [44-46]. Indeed, grafting method is classified into three types: grafting to or grafting onto, grafting from and grafting through (Figure 2). In brief, ‘grafting to’ method monomer chains are attached into reactive end-groups of the polymer backbone. In ‘grafting from’, conducting polymer backbone functionalized with initiation sites acts as macroinitiator, from which the side chains are grown afterwards, and ‘Grafting through’ method involves synthesis of macromonomers after polymerization into polymer backbone.[47, 48]

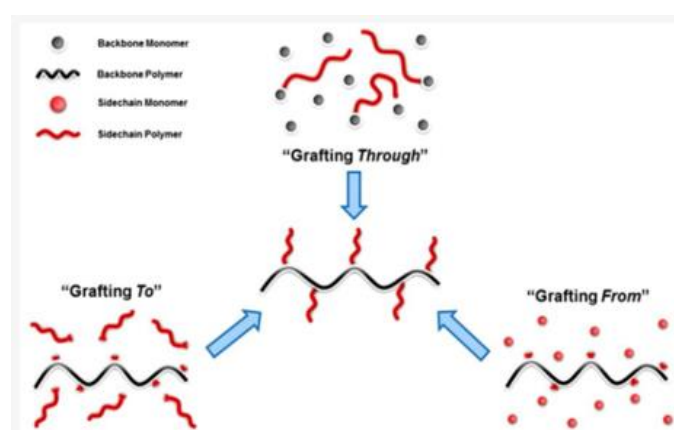


Figure 5 General classification of grafting mechanism [49]

1.3 Polymer-metal adhesion

The manufacture of Tetra Pak food containers is strongly dependent on the adhesion property between polyethylene and aluminum, so it is necessary to study what exactly the adhesion is and how to achieve it between different materials. Adhesion is the interatomic and intermolecular interaction at the interface of two dissimilar surfaces, which leads to cling them together by intimate interfacial contact such that mechanical force or work can be transferred across the interface [50]. The adhesion between polymers and different materials is a very complex subject that includes

interdisciplinary such as surface chemistry, physics, rheology, polymer chemistry, stress analysis, polymer physics, and fracture analysis [51]. The adhesion between metals and polymeric materials plays a major role in many industrial applications, especially food packaging and processing applications. Describing the mechanism of adhesion in simple terms is difficult due to the complexity and diversity of theories that explain this topic. Then, two common mechanisms or theories for adhesion phenomena between polymer-metal at the interfaces will be explained in this research, which are : mechanical coupling or interlocking , and thermodynamic mechanism of adhesion.

In the mechanical coupling or interlocking mechanism, the adhesion occurs by penetration of adhesives into the pores, cavities, and other surface irregularities on the surfaces of the materials to be bonded together, which resulted creation an adhesive bond strength from the “mechanical interlocking” of the adhesive and the adherends [51-53]. In addition, mechanical interlocking is a surface characteristic that studies the adhesion forces at the microscopic or macroscopic levels, not the molecular level [53]. However, adhesives frequently form stronger bonds to porous rough surfaces than they do to smooth surfaces [51-53].

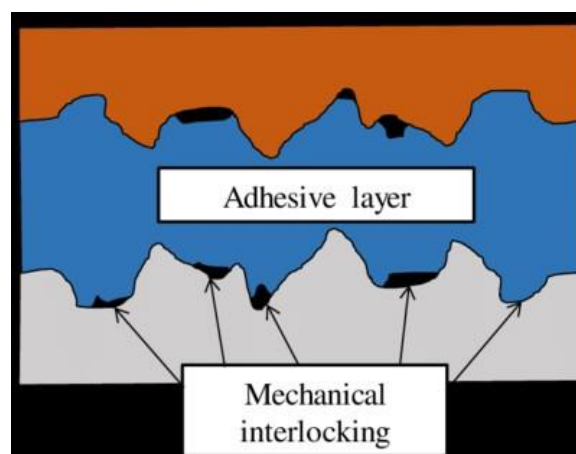


Figure 6 Mechanism of mechanical interlocking [54]

The thermodynamic mechanism of adhesion is distinguished from other mechanisms that it does not require a molecular interaction for good adhesion, only an equilibrium

process at the interface [55]. This mechanism is based on the wettability property by applying a polar liquid drop into the horizontal homogeneous solid surface to measure the angle created by the liquid at the three-phase boundary, where a liquid, gas, and solid intersect, this angle is known as the contact angle (θ_c). This property corresponding with surface tension and the surface free energy [51]. In fact, when θ_c is small (less than 90 degrees) this indicates that there is a strong attraction between the liquid and the solid substrate, and hence high wettability property (hydrophilic) of the solid surface. On the contrary, when the attraction between the liquid and the solid substrate is weak, a large θ_c is obtained (greater than 90 degrees), which confirms that the solid surface has poor wettability (hydrophobic) property [56].

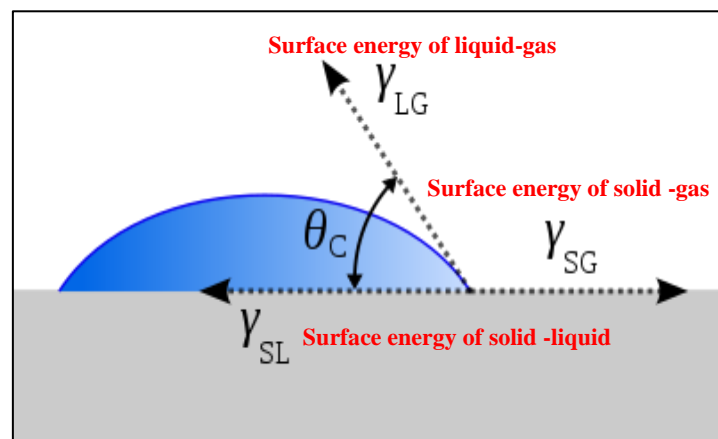


Figure 7 Schematic of dynamic contact angle at solid-liquid-gas contact line [57]

1.4 Problem statement

Laminates consisting of combination of low-density polyethylene (LDPE) and aluminum (Al) foils are widely utilized in many applications, especially in food packaging (Tetra Pak containers, e.g.), since LDPE has been contributed to achieve recognizable developments in the field of food packaging due to its unique properties. However, bonding strength (adhesion) between LDPE and Al components is a crucial for a final application in order to suppress a leakage of liquids from containers. The adhesion between LDPE and Al is inherently very low due to hydrophobic character (low wettability) of LDPE. On the other hand, the structure of LDPE, particularly degree of branching, degree of crystallinity and molar mass also plays an important role in interfacial adhesion. The target of this thesis is to explore a potential of various grades of LDPE produced by QAPCO for LDPE/Al laminates production in the respect of their inherent structure and surface characteristics.

1.5 Research objectives

The main objectives of this work can be divided into two domains, as follows:

- I. Study the changes in the surface characteristics including wettability, chemical and elemental compositions, and roughness of QAPCO LDPE grades to study their applicability in Tetra Pak containers after surface treatment with corona discharge, and radical grafting using different molecular weights of polyethylene glycol derivatives, and combination of these two surface modification techniques.
- II. Examination the adhesion quality of LDPE to Al before/after LDPE surface modification, using two techniques: mechanical peeling test and thermodynamic work of adhesion. The purpose of this to manufacture an adhesive joint of LDPE/Al multilayers that is used in food packaging and processing applications (e.g. Tetra Pak containers).

CHAPTER 2: LITERATURE SURVEY

2.1 Surface modification techniques of hydrophobic polymers

In previous studies, different approaches of modifying the polymers surfaces were discussed in order to increase the adhesion forces to different materials (metals, other polymers, etc.). Therefore, in this research two common approaches were used in surface modification of LDPE , which are : chemical modification by grafting active polar monomer into the polymer backbone and plasma treatment using corona discharge in separate to find out the most effective ones in surface treatment. Then, a new approach for modification LDPE film was studied, by combination of cold plasma treatment (corona radiation) with graft additives or radicals into the surface, to investigate the influence of plasma treatment on surface properties of the grafted samples.

2.1.1 Corona discharge

In the industrial level, corona plasma discharge is a preferred cold plasma technique in surface modification of polyolefin. It promotes surface activation which leads to enhance wetting and adhesion characteristics for applications that related with adhesive bonding and printing [58] [59]. It is characterized by fast in operation and completion (few seconds for treatment), cost effective (low cost), easily adapted to in-line operations [10], and environmentally friendly so no need to use aggressive polluted chemicals during operation [60]. Corona discharge occurs when ambient air molecules are ionized at the atmospheric pressure and the room temperature into charged particles such as electrons and ions. A high electric potential difference is formed between two asymmetric conductive electrodes (high-potential electrode and a grounded electrode) separated by a gap containing air. This creates a large electric field that accelerates the charged particles toward the polymer surface, which leads to incorporation of reactive

oxygen-rich functional groups on the surface such as carbonyl, hydroxyl, hydroperoxides, aldehydes, ethers, esters, etc. into the amorphous regions of the surface by etching and functionalization processes. The formed functional groups increase the polar part of surface energy and thus also the overall surface energy. Consequently, the polymeric surface is oxidized, its surface roughness and wettability increase, and finally remarkably higher adhesion with other materials [59, 61-63]. The dielectric barrier which is made of ceramic material and covers the ground electrode to avoid spark discharge, reduce charge leakage, and improve the electric field (as stored electrons and charges).[64, 65]

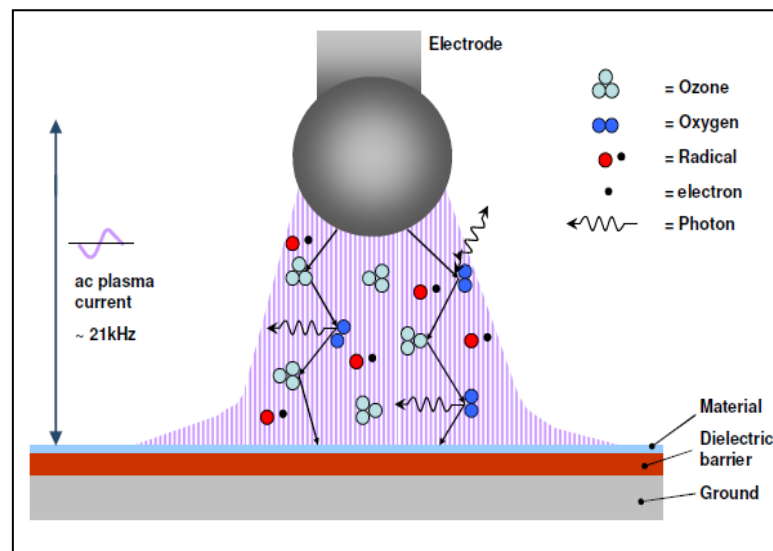


Figure 8 Corona discharge configuration

Sellin *et al.* studied the changes in the surface compositions of polypropylene films (PP) after treating their surfaces with atmospheric pressure corona discharge at different treatment times (up to 120s). They found incorporation of oxidized polar groups mainly, C=O, C-O and -OH, on the corona-treated PP surfaces according to Fourier transform infrared spectroscopy (FTIR) measurements. Also, they observed remarkable changes in terms PP morphology and surface structure by atomic force microscopy (AFM) analysis. Once the surface was exposed to corona discharge radiation, it was

noticed that the surface roughness increased along with formation of small droplets on the PP surface topography. They interpreted this the surface treatment with corona discharge leads to the polymer chain scission, due to formation oxidative polar groups on the treated surface. As a result, as surface modification continues, polymer chains become shorter, thus the molecular weight of the formed species on the surface are reduced, and finally the liquidity of modified surfaces is increased which results in large droplets. In addition, Sellin *et al.* demonstrated an enhancement in the surface wettability or hydrophilicity of the treated PP film according to contact angle measurements. A sharp decrease in the contact angle between the polypropylene and water (used as testing liquid) interface was recorded from 90° up to 54° after two seconds of the surface treatment. [66]

Pascual *et al.* studied the effect of corona discharge on the surface properties of LDPE films containing small quantities of ethylene-vinyl acetate (EVA) copolymer with the aim of improving stability. LDPE surfaces were treated at constant treatment speed (15 m/min), same treatment time (9 sec), and various working power range at max. 1 kW. Pascual *et al.* observed presence of oxygen containing functional groups such as carbonyl groups [C=O], and ester groups [O=C–O–C] on the LDPE films after treated their surface with corona radiation as demonstrated by FTIR spectrometer . Pascual *et al.* evaluated the wettability of the treated LDPE surfaces using contact angle test, where they concluded that with the increase in the plasma operating power, a decrease in contact angle between the LDPE surface and the testing liquid , and consequently the surface wettability was achieved.[58]

Popelka *et al.* examined the influence of corona discharge on the surface properties of Low-density polyethylene (LDPE) with the aim to adhere to Aluminum foil (Al) to create LDPE/Al laminate that is used in food packaging purposes. They treated both

LDPE sheet and Al foil separately using corona discharge at different time periods (1s, 3s, 5s, 7s, 10s). Then different characterization tools such as scanning electron microscopy (SEM), and Fourier transform infrared (FTIR) were employed to investigate the changes in the surface morphology and roughness. SEM images showed that the LDPE surface roughness increased slightly after 1 s of the surface treatment, nevertheless a noticeable change in surface roughness was observed after 7s of treatment. This generally refers to the formation of polar groups on the LDPE surface once exposed to the radiation generated by corona discharge. FTIR spectra observed that the intensity of the peak absorbance that corresponding to oxygen-containing functional groups such as O=C=O, C-O, C-N, and -OH increased with increasing the duration of surface treatment. In addition, Popelka *et al.* provided a detailed study on the change in wettability property with respect to both LDPE and Al surfaces using contact angle optical measuring system. Three different polarity testing liquids (ultra-pure water, and ethylene glycol with purity $\geq 98\%$) were used, and all of them created a drop in the contact angle with LDPE as the surface treatment time increased. Thus, it can be confirmed based on the previous results that the adhesion strength between LDPE and Al was enhanced after applying corona continuous radiation to both LDPE and Al surfaces. Finally, Popelka *et al.* used peel resistance testing system to measure the adhesive bond strength of LDPE/Al laminate. 1kN load cell at 90° peeling angle was employed to separate the LDPE from the adhesive joint at slow speed rate of 10 mm/min. They found that the peel resistance (adhesive strength) increased significantly as longer the treatment time for both LDPE and Al surfaces by corona discharge.[67]

2.1.2 Chemical modification via grafting with PEG monomers

Polyethylene glycol (PEG) is a versatile hydrophilic polyether that has many applications, mostly in the medical and biomedical applications due to its non-toxicity,

, biocompatibility, and high solubility in most solvents [68, 69]. It can be immobilized onto the polymer surfaces using various techniques as physical adsorption, grafting process, covalent grafting, blending etc. [70-73]. It is synthesized *via* chain-growth ring-opening polymerization of ethylene oxide in the presence of methanol or water as an initiator [74] . PEG is available as linear or branched chain polymers with an oxyethylene (–O-CH₂-CH₂–) repeating units [70, 75] . The molecular weight of PEG plays a considerable role in specifying its properties , where PEG is also known as polyethylene oxide (PEO) when it presents in the form of a solid crystalline powder with molecular weight greater than 20000 g / mol, while PEG exists as viscous liquid or waxy solid with molecular weights below 20,000 g / mol [70]. Both PEG and PEO compounds are soluble in both aqueous and organic solvents [76, 77]. Although PEO and PEG have an O-(CH₂)₂ monomer, they differ in terminal groups, as shown in Figure 7. Recently, many studies have been focused on development the surface modification of hydrophobic polymers *via* grafting by PEGs.

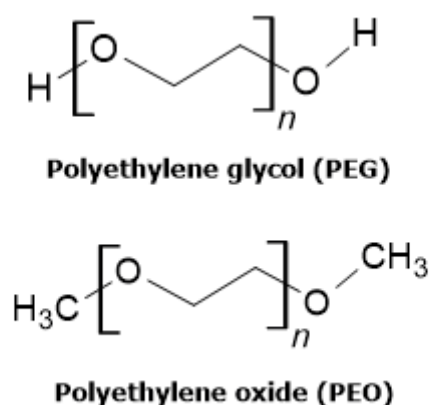


Figure 9 Chemical structure of PEG and PEO polymers

Chen *et al.* aimed to improve the surface properties of a blended film made of Linear low-density polyethylene (LLDPE) and styrene-maleic anhydride copolymer (SMA) by immersing into aqueous solution of polyethylene glycol (PEG) with molecular weight 400 g/mol at room temperature for a week in order to achieve the grafting

reaction. FTIR spectra showed that LLDPE/SMA film with 20% SMA after immersion in PEG solution, caused to appear characteristic absorption band of ester carbonyl group vibration. Furthermore, they found the water contact angle of the LLDPE/SMA blended film decreased as the concentration of PEG grafted onto its surface increased, which promotes an effective improvement in the surface wetting properties of the LLDPE/SMA blend. This is due to generation of oxygen-containing functional groups on the treated surface, which was proven by FTIR analysis. [78]

Liu *et al.* worked on surface modification of polyester urethane (SPEU) films with different molecular weights of polyethylene glycol (PEG) compounds $M_n = 1200, 2400$ and 4000 g/mol, based on high grafting density for biomedical purposes. It was found that when SPU is used in the manufacture of medical blood-contacting materials, the surface of SPU films leads to significant protein adsorption and platelet adhesion by activating the coagulation pathway in the long-term, thus leads to form the microscopic thrombi. Therefore, Liu *et al.* modified the SPU surface by grafting poly (ethylene glycol) (PEG) on its surface, since PEG has the ability to prevent protein adsorption and platelet adhesion due to its low interfacial free energy with water, unique solution properties, hydrophilicity, high chain mobility, and steric stabilization effect. The grafting polymerization process of SPEU-PEG, which was carried out by the researchers, involved of three consecutive chemical treatment steps under mild conditions. Firstly, surface treatment of SPEU film with 1,6-hexanediisocyanate (HDI) solution using allophanate reaction in order to introduce -NCO groups onto the surface. SPEU film was completely immersed into 10% HDI solution for 3 h at room temperature, whereas HDI solution was prepared in advance by dissolving small amounts of HDI and Dibutyltin dilaurate (DBTDL) into anhydrous toluene. Thereafter tris(2-aminoethyl)amine (TAEA) was dissolved into anhydrous toluene and the SPEU-

NCO film was dipped in it with gentle shaking for 6h to attach -NCO groups on SPEU film with -NH₂ groups from TAEA to immobilize -NH₂ on the surface. Finally, after washing PEU-NH₂ film with anhydrous toluene to eliminate excessive TAEA from PEU-NH₂ surface, different molecular weight of PEG was grafted onto the SPEU surface by Michael addition. PEU-NH₂ was totally immersed into PEG-absolute ethanol solution for 12 h at room temperature with stirring to achieve strong interlink between terminal C = C bond of monoallyloxy PEG and -NH₂ group on the film surface. The results showed that with increasing the molecular weight of PEG, there was a significant decrease in the water contact angle between the water / PEG-g-SPEU interface, which indicates increase in the surface energy and polarity, and thus strongly hydrophilic SPEU surface. Also, this can be attributed to high grafting density of PEG on the SPEU-PEG surface. Furthermore, Liu *et al.* found that the amount of adsorbed protein on the PEG-g-SPEU surfaces decreased by more than half the protein adsorption value of the blank SPEU surface, indicating a better blood compatibility of SPEU-PEG surface. Last but not least, the platelet adhesiveness was studied through SEM micrographs. Platelet aggregation was observed on the blank SPEU surface, whereas after PEG grafting on the SPEU surface the amount of adherent platelets was greatly de-creased. This proves that the modified surfaces have better adhesion property of anti-platelets, due to hydrophilic nature and low blood and plasma proteins interfacial energy as a result of presence of PEG on the surfaces, and then leads to inhibit the platelet adhesion [79]

CHAPTER 3: METHODOLOGY

3.1 Materials

Three different grades of low-density polyethylene (LDPE) from Qatar Petrochemical Company (QAPCO, Qatar) were used to compare with the LDPE competitor (or commercial) LDPE that is used in Tetra Pak industry. They are marked with the identification codes: LDPE EC1-041, LDPE EC1-049, and LDPE EC-02. The materials in granular form were hot-pressed into thin transparent sheets using mounting hot press machine (Carver 3895, USA). The basic physical properties and potential uses for LDPE grades are summarized in Table (1). LDPE sheets were bonded with aluminum (Al) foils (GLAD[®], China) to produce a coherent adhesive joint (LDPE/Al laminates), which achieving the main purpose of this work.

Table 1 The physical properties and potential uses of the tested LDPE grades

Polymer properties	EC01	EC02
Density @ 23 °C (ASTM D-1505)	0.918 g/cm ³	0.923 g/ cm ³
Melt flow index 190°C/2.16 kg (ASTM D-1238)	8.0 g/10 min	4.0 g/10 min
Crystalline melting Point (ASTM E-794)	105 °C	108 °C
Recommended uses	Extrusion coating at high speed	Extrusion of very high clarity blown and cast films

In addition, the following materials were used:

- Acetone (C₃H₆O, molar mass M = 58.08 g/mol, density D= 0.787-0.791 g/cm³ at 20°C/4°C, min.99.8% assay by G.C. method) was provided from Scharlab S.L., Spain to remove any impurities or contaminants from the LDPE and Al surfaces prior applying the surface treatment.
- For surface modification of LDPE surfaces *via* grafting, PEG waxy solid-state compounds with different molecular weights (M) : 1000 g/mol (Fluka Chemika,


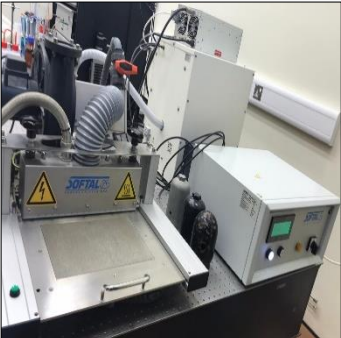

Switzerland), and 6000 g/mol (Merck KGaA, Germany), as well as solid-state PEO with $M = 300,000$ g/mol (Sigma-Aldrich corporation, USA) were used to increase the hydrophilicity of LDPE surfaces.

- For the wettability investigation of LDPE surfaces, Ultra-pure water (Purity $\geq 99\%$, water purification system Direct-Q[®], France), formamide (Purity $> 98\%$, FLUKA[™], Belgium), ethylene glycol (Purity $\geq 98\%$, FLUKA[™], Belgium) were used as testing liquids with different surface tension to measure the contact angle when liquid–vapor interface meets a solid substrate, as well as to determine the changes the total surface free energy and its components: polarity and dispersion of the pristine, corona treated, radical grafted *via* PEG/PEO chains, and corona treated PEG/PEO grafted LDPE specimens.
- Distilled water was used to dissolve PEG/PEO powder and prepare aqueous solutions at specific concentrations.

3.2 Experimental apparatus/equipment

The equipment/devices that were employed in preparing the LDPE specimens, applying the surface modification, and testing the interfacial adhesion in LDPE/Al bonded joints are illustrated in table 2.

Table 2 List of used equipment

Name of the equipment	Illustrative image	The manufacture company	Application(s)
Mounting Hot Press Machine		Carver 3895, USA	<ul style="list-style-type: none"> - To convert LDPE granules into thin sheets. - To prepare the LDPE/Al laminate
Corona Plasma Discharge		SOFTAL, Germany	Cold plasma system that was employed in surface modification of the LDPE before lamination
Contact angle measuring system (OCA 35)		DataPhysics Instruments, Germany	To measure the degree of wetting (wettability) of LDPE surfaces before and after modification

Peel tester LF-Plus



LLOYD
Instruments™,UK

To determine the adhesive strength
at 90° peeling between LDPE and
Al sheets

3.3 Experimental procedure

This work focused on studying the potential techniques that can be used in improvement the surface properties of different grades of LDPE with the aim to increase their adhesion to Al foils, and thereafter form LDPE/Al adhesive joints that are involved later in industrial applications, such as food packaging. LDPE surfaces have inert nature and characterized as non-polar hydrophobic tendency, which cause the adhesion between LDPE and Al to be relatively low. The surface modification techniques employed in this research include corona discharge followed by grafting of poly PEG/PEO active groups on LDPE surfaces. Moreover, the adhesion quality of polyethylene (PE)/aluminum (Al) laminates was assessed by 90-degree peel test. It should be pointed out that untreated (pristine) LDPE samples were utilized as reference samples in order to examine the changes in surface properties before and after modifications.

3.3.1 Preparation of LDPE thin sheets and LDPE-Al laminate

The LDPE granulates were converted into thin sheets using hydraulic mounting press machine (Carver 3895, USA). Ten grams of LDPE granules were placed between two transparent polyester sheets inside two highly polished stainless-steel plates, with a concern that granules were positioned adjacent to each other and on one level. After that, all the previously prepared were entered between the upper and lower molding

plates of the hydraulic press machine, these plates are fabricated of high carbon steel since the operations related to pressing and heating are done in between them. After turning on the machine, the required conditions to conduct the experiment were specified. LDPE granules were heated up into a temperature slightly higher than the melting temperature ($160^{\circ}\text{C} = 320^{\circ}\text{F}$). Once the desired temperature was reached, one-ton load was applied into the LDPE granules for two minutes, to convert these granules into a thin sheet under the influence of applied temperature and pressure. Finally, the prepared LDPE sheet was cooled down gradually until room temperature. The thickness of the sheets were measured by Vernier caliper and found approximately $205\ \mu\text{m}$, $270\ \mu\text{m}$, $290\ \mu\text{m}$, and $320\ \mu\text{m}$, for competitor, EC01-041, EC01-049, and EC02 LDPE grades respectively .

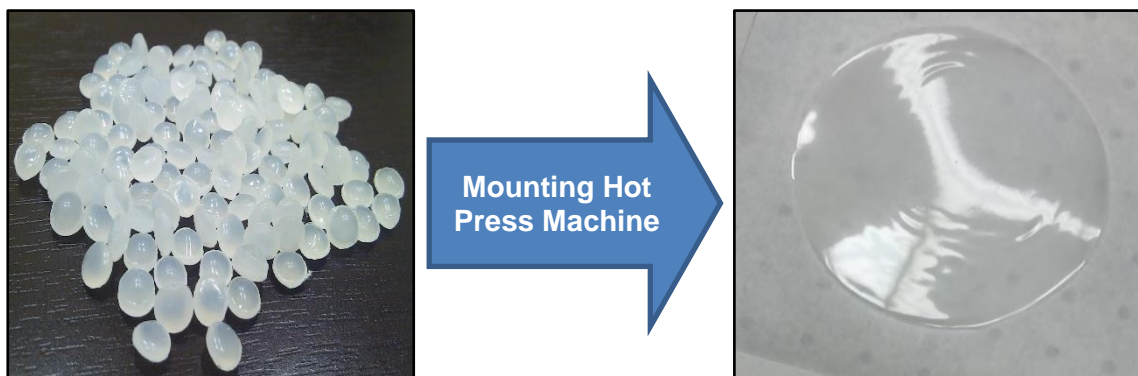


Figure 10 LDPE thin sheet preparation

The LDPE/Al laminate was fabricated by mounting press machine with almost the same steps as LDPE sheet preparation. LDPE untreated/treated sheet was placed directly on the shiny side of Al foil, then gradually heated up until reached temperature of $160\ ^{\circ}\text{C}$ followed by two tons compression molding was applied for two minutes into the LDPE/Al combination, and finally cooled down the LDPE/Al laminate into room temperature.

3.3.2 Pre-treatment of LDPE sheets

Both sides of the LDPE sheet were completely immersed in a Petri dish containing an organic solvent such as acetone under room temperature for short time (few seconds) to remove all undesirable contaminants from the surface such as soot, dust, oil, and other impurities. Then LDPE sheets were left to completely dry at room temperature prior to surface treatment. This step was also applicable to Al foils for the same purposes.

3.3.3 Surface modification of LDPE surface using corona discharge

The surface properties of LDPE surfaces such as morphology, wettability, functionalization, bonding, and interfacial adhesion were modified using corona discharge. Corona plasma system (Softal, Germany) was employed under moderate experimental conditions, which include room temperature (20–22°C), and atmospheric pressure (101.325 kPa). In addition, this experiment was operated at nominal power supply (300 W), high frequency (typically 17.20 kHz) of the voltage provided between the discharge and grounded electrode that were separated by 1.5 mm gap distance. The LDPE surfaces were treated from both sides with corona radiation at various treatment times (1, 3, 5, and 7s) in order to study the relationship between the duration of the applied corona discharge on the exposed surfaces and the enhancement in the surface properties and hence adhesion strength of the LDPE/Al laminates. It should be emphasized that high-efficiency ozone gas (O₃) was used as the active feed gas derived from ambient air which is responsible for homogeneous surfaces treatment of LDPE. This system contains a catalytic ozone removal system ensuring a safe working environment.

3.3.4 Grafting of PEG/PEO onto LDPE surfaces beside corona discharges

For surface modification of LDPE surfaces *via* grafting, two solid-state PEG compounds with different molecular weights (M) : 1000 g/mol and 6000 g/mol, as well as PEG powder with M=300,000 g/mol were used [Figure 11]. The untreated and plasma-treated LDPE EC01-049 specimens were completely immersed into specific concentrations of PEG/PEO- based aqueous solutions at room temperature for 24 h to achieve grafting onto LDPE surfaces as shown in Figure 12. For plasma-treated PEG/PEO-g-LDPE specimens; the optimal corona treatment time was 5 s, which was associated with the best achieved wettability. The aqueous solutions of PEG/PEO were prepared by adding specific amounts of PEG/PEO gradually into a particular volume of distilled water with continuous stirring until the PEG/PEO particles were completely dissolved into the water and then dilute homogeneous solutions were obtained. After the grafting 'onto' process, LDPE specimen was rinsed with successive batches of distilled water immediately after extraction from the solution, to remove unreacted species from the surface. Thereafter, it was left to totally dry at room temperature before fabrication of LDPE/Al laminate. Six PEG/PEO based aqueous solutions were tested in this work, regarding two different concentrations per each molecular weight. The purpose of this experiment is to investigate the influence of changing the molecular weight of PEG/PEO chains, and concentration of prepared PEG/PEO solutions on the surface characteristics of coated LDPE films. The concentrations of the solutions used were as follows: 1.5 wt.%, and 10.0 wt.% concentrations for both 1000M PEG and

6000M PEG, and 1.5 wt.% and 5.0 wt.% (maximum solubility) for 300,000M PEO.

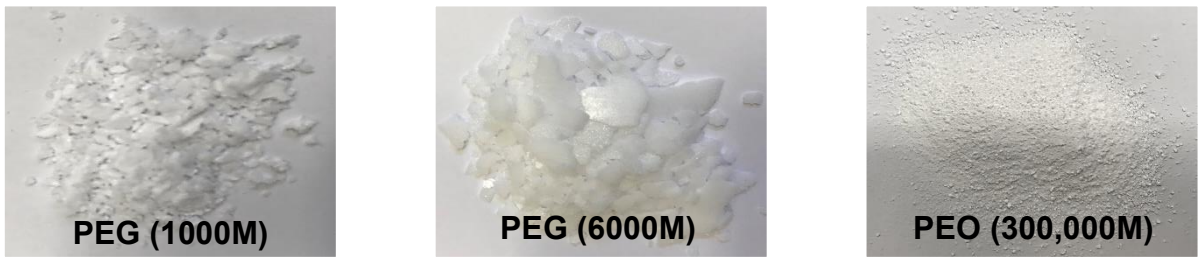


Figure 11 Solid-state pure polyethylene glycols

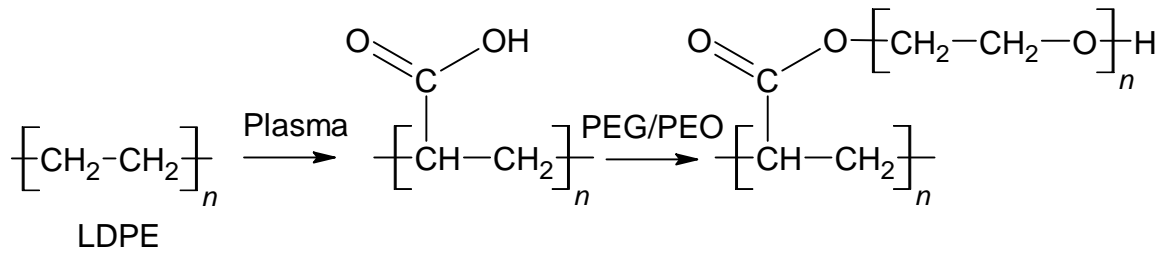


Figure 12 Scheme of proposed grafting mechanism of PEG/PEO onto corona-treated LDPE.

3.3.5 Grafting efficiency (%GE) calculation

Grafting efficiency (%GE) is defined as the percentage of the amount of the grafted monomer which is linked into the polymer backbone to the total amount of the free polymer. %GE values of the PEG/PEO-g-LDPE specimens were calculated gravimetrically using Equation (1)

$$\% \text{GE} = \left(\frac{m_1 - m_0}{m_0} \right) \times 100\% \quad \dots\dots(1)$$

Where; m_0 = the mass of the LDPE sample before grafting (g), m_1 = the mass of the LDPE sample after grafting with PEG/PEO chains (g).

3.3.6 Determination of surface wettability

The change in surface wettability or hydrophilicity of the untreated and treated LDPE specimens were investigated by measuring the contact angle of selected liquids deposited on the investigated surfaces. In this work, three testing liquids with different surface tension and polarity were employed in dynamic contact angle measurements,

which are: ultra-pure water, formamide and ethylene glycol (see Table 3). System OCA 35 (Dataphysics, Germany) was used in the contact angle measurements. This system is connected to an optical video-base imaging system linked to high-resolution USB camera (up to 2200 images/sec). According to the sessile drop method, 3 μ L volume droplet of each testing liquid was deposited softly with constant flow rate of 2 μ L / s on relatively small LDPE samples with the dimensions of 8 cm length x 2 cm width. Then, the contact angle was measured after 3 s to ensure that the liquid droplet spreads evenly and completely over the surface, while thermodynamic equilibrium was achieved. At least five separate readings for each testing liquid were taken to obtain one representative average contact angle value that is used in the calculation of solid/liquid interfacial tension based on the Owens-Wendt-Rabel-Kaelble method (OWRK-model). OWRK-model expresses the interfacial interactions along the solid and liquid molecules in term of three components, the total surface free energy (γ) and its components: polar (γ^p) and dispersive (γ^d) components, by the Equation (2)

$$\gamma_{sl} = \gamma_s + \gamma_l - 2 \left(\sqrt{(\gamma_s^d \cdot \gamma_l^d)} + \sqrt{(\gamma_s^p \cdot \gamma_l^p)} \right) \dots\dots(2)$$

Table 3 Surface free energy and its components of the testing liquids at 23 °C

Testing liquid	Surface energy, γ_l (mN/m)	Dispersive, γ_l^d (mN/m)	Polar, γ_l^p (mN/m)
Water	72.1	19.90	52.20
Formamide	56.90	23.50	33.40
Ethylene glycol	48.00	29.00	19.00

3.3.7 Determination the adhesion strength of LDPE/Al laminate

The 90° peel test as an appropriate method was employed for the evaluation the adhesion characteristics between plastic (LDPE) and elastic (Al) components that form together a coherent laminate. Peel tester LF-Plus (Lloyd Instruments, UK) based on

ASTM D6862 standard test method was employed in the adhesion strength measurements. This system is connected to NEXYGENPlus testing software which displays the results as numerical values or representative graphs. Laminated LDPE/Al strips with dimensions approximately of 8 cm height and 2 cm width were attached tightly on an acrylic two sided tape (3M 4910k,VHBTM) prior the starting the test. Then the peel strength (the force per unit width of the laminate) was measured under dynamic conditions: 1kN load cell was applied at 90° angle peeling on the specimen, operated at slow speed rate ($v=10$ mm/min) to ensure the applied peeling force is evenly distributed over the surface, and the test time was set at a maximum of 360 s to ensure that LDPE ultra-thin layer was completely separated from the Al foil. The peel resistance was evaluated from 10 mm - 50 mm distance of the LDPE/Al laminate. Following to Standard Test Method for 90 Degree Peel Resistance of Adhesives (ASTM D6862) between flexible material (LDPE) and rigid material (Al); 4-5 separate readings of LDPE-Al adhesives were taken to acquire one average value of the peel resistance, and subsequently compared with the work of adhesion computed from contact angle measurements.



3.3.8 Calculation of the work of adhesion

Moreover, the strength of adhesion between the polymer-metal at interfaces can be estimated through the thermodynamic work of adhesion (W_{12}) calculations based on the surface wettability measurements. W_{12} for a solid–solid combination is defined as the reversible thermodynamic work (energy change per unit area) that is required to separate two adherent materials to form a laminate from the equilibrium state into a separation distance of infinity [80].

In this work, W_{12} of untreated, plasma treated and modified LDPE in the LDPE/Al laminate adhesive joints were calculated from contact angle measurements and depending on the polarity and dispersion values of the surface energy by Young – Dupré equation (eqn.3) ,as follows [81]:

$$W_{12} = \gamma_1 + \gamma_2 - \gamma_{12} \dots \dots \dots (3)$$

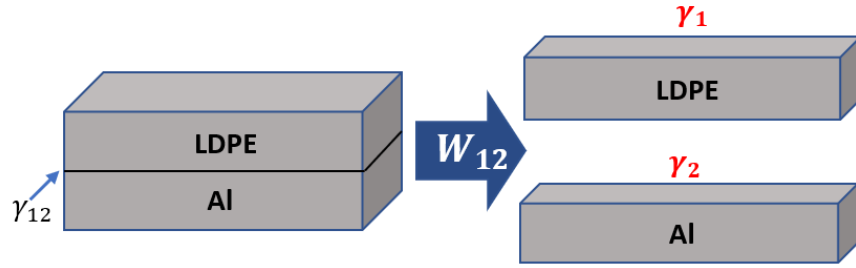
Where γ_1 is the surface energy of LDPE , γ_2 is the surface energy of Al, γ_{12} is the interfacial energy between the LDPE/Al (solid–solid interface) and can be determined by the following equation.

$$\gamma_{12} = \gamma_1 + \gamma_2 - 2(\gamma_1^p * \gamma_2^p)^{\frac{1}{2}} - 2(\gamma_1^d * \gamma_2^d)^{\frac{1}{2}} \dots \dots \dots (4)$$

by substituting Eq. (4) into Eq. (3); the work of adhesion (W_{12}) is obtained by Fowkes’ theory as follows:

$$W_{12} = 2[(\gamma_1^p * \gamma_2^p)^{\frac{1}{2}} + (\gamma_1^d * \gamma_2^d)^{\frac{1}{2}}] \dots \dots \dots (5)$$

where subscripts ‘1’ and ‘2’ refer to LDPE and Al respectively; the superscript ‘d’ represents to the non-polar/dispersive contribution; and the superscript ‘p’ refers to the polar contribution to the surface free energy.



3.4 Characterization and analytical techniques

3.4.1 Investigation of the thermal properties

Differential Scanning Calorimetry (DSC)

In this work, differential scanning calorimetry (DSC-8500, PerkinElmer, USA) was employed in measuring the specific heat capacity as a function of temperature to investigate the melting temperature (T_m) and crystalline temperature (T_c) of the LDPE pristine grades. Enthalpies of melting (ΔH_m) and crystallization (ΔH_c) were measured from the DSC heating and cooling curves respectively, where temperature was ranged from 30°C to 150 °C at the same heating rate of 10 °C/min for all LDPE grades. High-purity nitrogen was used as a DSC standard purge gas in order to operate the system. In addition to the above, the results obtained were later used in the degree of crystallinity, X_{DSC} (%) calculations of each LDPE grade. It was calculated as measured enthalpy of the melting peak (ΔH_m) corresponding to the actual heat of melting of 100% crystalline LDPE ($\Delta H_{actual} = 290$ J/g as addressed in the literature)[82]. The degree of crystallinity (%) was evaluated using Equation (6)

$$X_{DSC} (\%) = \frac{\Delta H_m}{\Delta H_{actual}} \times 100\% \dots\dots(6)$$



Figure 15 DSC-8500, PerkinElmer[®] instrument

3.4.2 Surface morphology analysis

Scanning electron microscopy (SEM)

The changes in surface morphology and roughness of LDPE samples before and after surface modification were investigated by scanning electron microscopy (FEI Quanta 200 ESEM, Thermo Fisher Scientific [™], USA). The LDPE specimens were observed at high magnification: 5000x, 10000x, 20000x, 40000x, and at high spatial resolution in order to achieve high quality of the observed images. The working distance (WD) between the source of electrons and the exposed surface of the sample was set within the range of 4.5-5.1mm. Furthermore, SEM system was operated with moderate acceleration voltage equals to 5.0 kV. Then, the electrons were transferred *via* high-speed beams and hit the sample. The reflected electrons were detected by SEM, and the absorbed ones interact with the specimen to provide a semi-quantitative elemental analysis by EDX.

Atomic force microscopy (AFM)

The three-dimensional (3D) changes in the surface topography and roughness of the pristine, corona treated, PEG/PEO grafted LDPE EC01-049 samples were determined using atomic force microscopy (AFM). AFM topographical images were carried out by an MFP-3D AFM device (Asylum Research, Abingdon, Oxford, UK) using AC160TS

highly conductive doped silicon probe with conical shape (Veeco model, OLTESPA, Olympus, Tokyo, Japan). This probe is covered with a thin reflex aluminum coating in order to prevent the light directed from the microscope lens towards the sample surface being scattered or lost. Furthermore, AFM Measurements were conducted under ambient conditions in the dynamic mode in air (AC mode) known also as tapping mode. This mode is preferred due it overcomes the technical problems which related with friction, adhesion, electrostatic forces that may appear after a plasma treatment and cause image data to be distorted [83]. AFM is an ideal tool to quantitatively measure the nanometric dimensional surface roughness and to visualize the surface nano-texture of the deposited film, *via* commonly parameter that describe the vertical dimensions of the surface, namely average surface roughness (Ra). Ra is defined as an arithmetic average of the height of the bothside rough irregularities in the direction perpendicular to the sample surface [84, 85].

3.4.3 Surface composition evaluation

Fourier-transform infrared spectroscopy (FTIR)

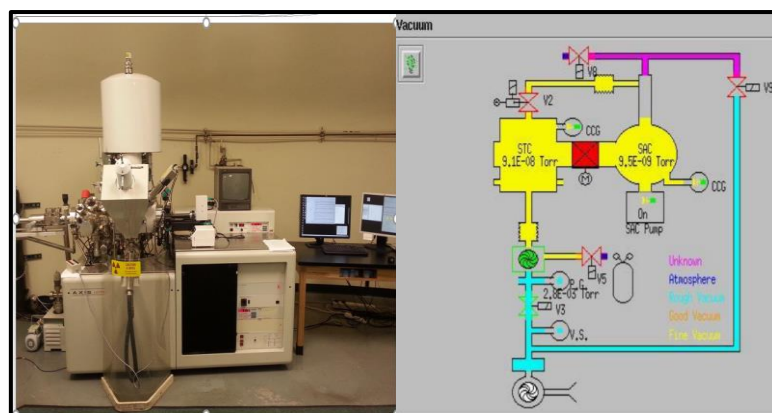
Fourier-transform infrared spectroscopy (Spectrum 400, PerkinElmer, USA) was employed to identify the changes in chemical composition of LDPE untreated /treated surfaces. FTIR spectra were recorded of the LDPE surfaces within a wavenumber range of 500-4000 cm^{-1} at spectral resolution of 4 cm^{-1} in the absorbance mode to collect 8 scans with aim to obtain accurate measurements.



Figure 16 Fourier-transform infrared spectrometer (FTIR)

X-ray photoelectron spectroscopy (XPS)

The elemental and chemical compositions of the untreated and treated LDPE specimens were evaluated using X-ray photoelectron spectroscopy (Axis Ultra DLD, Kratos Analytical ,UK). XPS spectra is measured by irradiating a monoenergetic X-rays to the surface, causing the emission of photoelectrons that are located within 10 nm from the surface. Thus, the kinetic energy of the electrons emitted from each element present on the surface is analyzed, and the spectrum is obtained as a plot of the number of detected electrons per energy interval versus their kinetic energy. Consequently, it can be said that each element has its unique spectrum. quantitative data is calculated based on the peaks formed by spectra of the individual elements according to the peak heights, areas, positions, and certain spectral features [86]



CHAPTER 4: RESULTS AND DISCUSSION

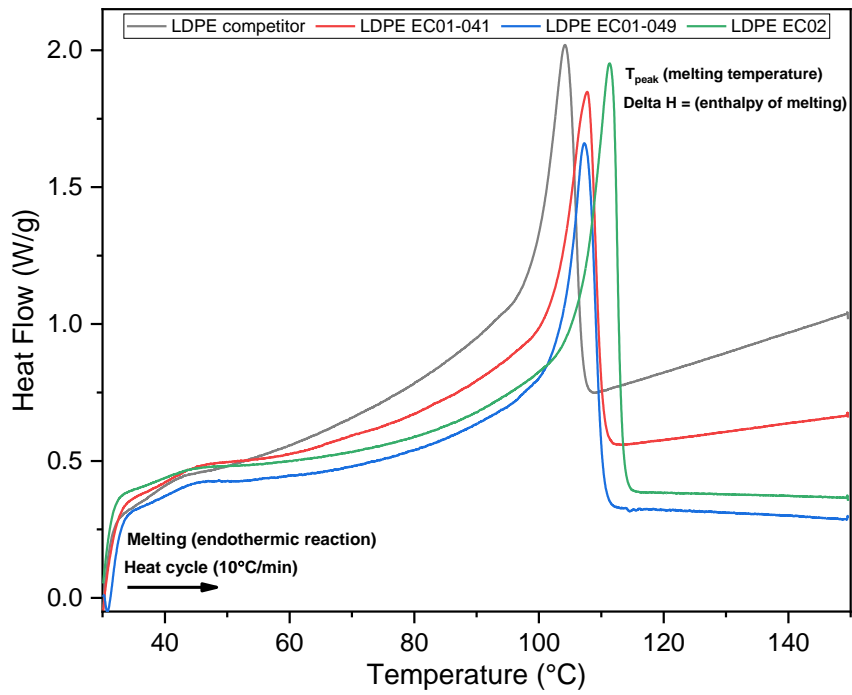
4.1 Thermal analysis of LDPE

Figure 18 shows DSC scans of the four pristine LDPE specimens: LDPE competitor, LDPE EC01-041, LDPE EC01-049, and LDPE EC02 within a range of 30°C-150°C to study the isothermal melting and crystallization behavior. It can be observed that all LDPE samples were heated with rate 10 °C/min starting from 30°C (room temperature) to reach the highest point of the curve (T_m) where all the solid LDPE were completely in molten state (it is rare for a semi-crystalline polymer to be present in a liquid state). T_m indicates to average melting point and was recorded as 104.02°C, 106.27°C, 106.47°C, 111.56°C for competitor, EC01-041, EC01-049, and EC02 respectively. Furthermore, the heat absorbed by the LDPE backbone from the surrounding to break the covalent bonds within its structure during the melting process is known as the enthalpy of melting (ΔH_m). ΔH_m values were determined from the area under the melting peak, and found within a range of 50-61 J/g for the LDPE grades (Figure 18(A)). After heating, molten-state LDPE specimens started to be cooled with the same heating rate (10 °C/min) to reach the lowest point in the crystallization curve which represents the average crystallization temperature (T_c). For LDPEs competitor, EC01-041, EC01-049, and EC02, T_c were recorded as 89.95°C, 91.75°C, 91.80°C, and 96.66°C respectively. At this temperature, LDPE structure converts from molten state into solid state with well-ordered portions that contain both crystalline and amorphous regions. Furthermore; the area under the crystalline curve defines as the heat or enthalpy of crystallization (ΔH_c), and found ΔH_c values estimated within the range of 52-66 J/g. Despite that, it was found that ΔH_c had higher value compared with ΔH_m , because large amounts of heat were emitted from the LDPE during cooling to transform the molten LDPE into solid structure with certain degree of crystallinity (Figure 18 (B)). In

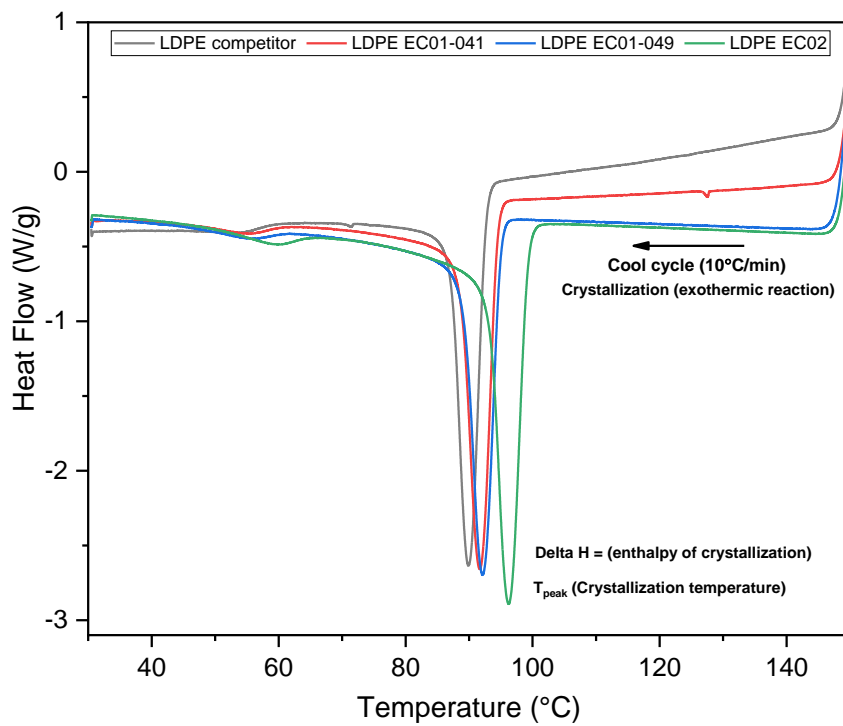
addition to the above, the degree of crystallinity, X_{DSC} (%) for each LDPE grade was calculated based on the enthalpy of melting (ΔH_m). Therefore, X_{DSC} percentages from the highest to the lowest were as follows: 19.40%, 18.06%, 17.41%, and 17.22% for LDPE EC02, LDPE competitor, LDPE EC01-041, and LDPE EC01-049 respectively. It can be seen that the X_{DSC} (%) values are very close, which indicates LDPE specimens have almost level of crystallinity. The low crystallinity degree indicates that LDPE branched structure consists mostly of amorphous regions surround by small crystalline regions (less perfect structure). These branching structures prevent the molecular chains from packing close together, and thus the density of the LDPE grades decrease. As a results; less rigidity of the polymer and decrease in stiffness, softening and melting points tensile strength, barrier to moisture and gases and resistance to oil and grease [87, 88]. The melting and crystallization temperatures as well as the related measured molar enthalpies of the tested LDPE grades are tabulated in Table 4.

Table 4 Melting and crystallization parameters for LDPE grades according to DSC measurements

LDPE grade	T_m (°C)	ΔH_m (J/g)	T_c (°C)	ΔH_c (J/g)	X_{DSC} (%)
Competitor	104.02	52.36	89.95	52.76	18.06
EC01-041	106.27	50.49	91.75	63.54	17.41
EC01-049	106.47	49.96	91.80	57.91	17.22
EC02	111.56	56.27	96.66	65.37	19.40



(A)



(B)

Figure 18 DSC (A) melting and (B) crystallization curves of LDPE specimens

4.2 Surface modification by corona discharge

4.2.1 Surface wettability analysis

The wettability refers to the ability of a liquid to maintain in contact with a solid substrate. This interface property is characterized by the contact angle (θ) created when a drop of liquid is placed on a flat, horizontal solid surface. Thus, the relationship between surface wettability and contact angle can be expressed as: the wettability of a surface increases as the contact angle gets smaller and vice versa. In this work, the contact angle measurements between LDPE surfaces and testing liquid with various tension and polarity were measured at variation in treatment times with corona discharge 0s (untreated), 1s, 3s, 5s, and 7s. As can be seen in Figure 19, a dramatic decrease in the contact angle values for all the LDPE grades was observed with increasing surface modification time. To illustrate this, the water contact angles decreased significantly from 97.66° , 74.74° , 72.33° , and 93.53° for untreated specimens into 57.87° , 62.34° , 59.82° , and 69.80° after 7s of surface treatment with corona radiation for competitor, EC01-041, EC01-049, and EC-02 respectively. The relatively high contact angle values of untreated LDPE surfaces refer to their hydrophobic, low wetting and non-polar nature. In contrast, the relative low values of contact angles of testing liquids for untreated EC01-041 and EC01-049 LDPE specimens compared with the other LDPE grades were probably affected by the processing additives as was confirmed by present of oxygen containing groups observed by FTIR and XPS. Therefore, surface treatment contributed to break the covalent bonds between carbon atoms within the LDPE surface to substitute by oxygen containing polar functional groups such as C=O, -OH, COOH, C-O-C, which resulted from the ionization of air molecules. Hence, increase in the surface wettability and polarity were achieved for all the corona-treated LDPE specimens. Moreover, it was observed that the untreated

LDPE competitor had the highest contact angle values compared to the rest of the polyethylene grades. This is because it has the largest amount of covalent bonds between carbon atoms, which consistent with the XPS results. However, it recorded the largest decrease in contact angles after surface treatment, which confirms the surface oxidation *via* air plasma. Finally, it was found that the lowest contact angles between the water and the LDPE surfaces were observed after 5s of corona treatment and as follows: 57.57°, 61.68°, 57.56°, 66.52° for competitor, EC01-041, EC01-049, and EC-02 LDPEs respectively, which means it is the optimum time for surface treatment with corona radiation.

Surface free energy (γ_s) and its derivatives polar (γ_s^p) and dispersive (γ_s^d) components were measured for untreated and surface-treated LDPE specimens with the aim to investigate the influence of corona surface treatment on the characteristics of solid–liquid interactions [89], as can be seen from Figure 20. The surface free energy and its components values were carried out based on the contact angle measurements, so it was concluded that the surface free energy is inversely correlated with contact angle of the testing liquid, which means the treated LDPE samples with relatively low contact angles had the higher surface energy values, due to incorporation oxygen-containing radicals and creation polar interactions on their surfaces as a result of surface functionalization by plasma radiation. This contributed to increase the polarity and reduce the dispersion (non-polar) values. Subsequently enhancement in the wettability

property was demonstrated for all LDPE grades.

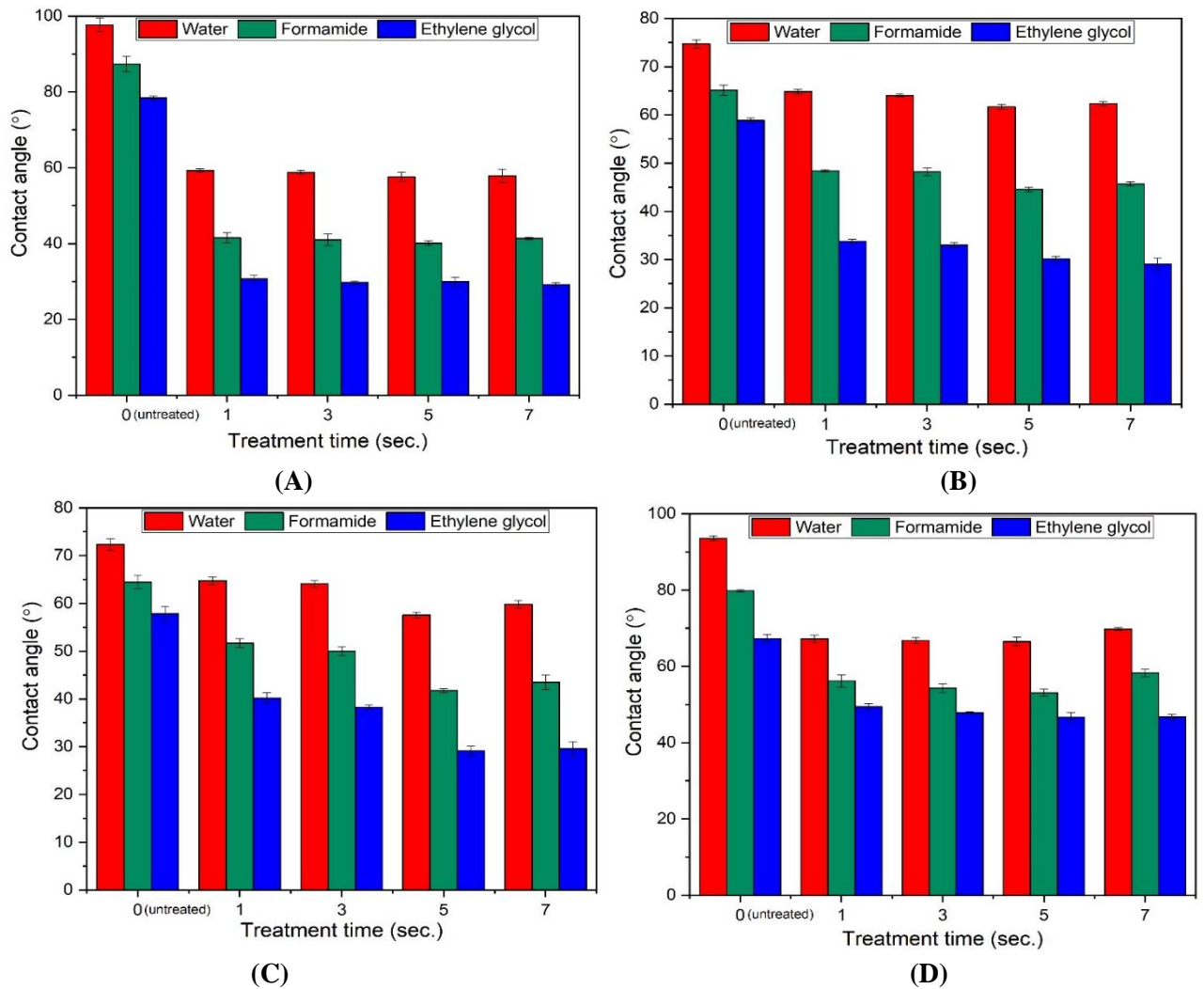


Figure 19 Contact angle (°) of LDPE samples vs. corona-treatment time (sec.).

(A): Competitor, (B): EC01-041, (C): EC01-049, (D):EC02

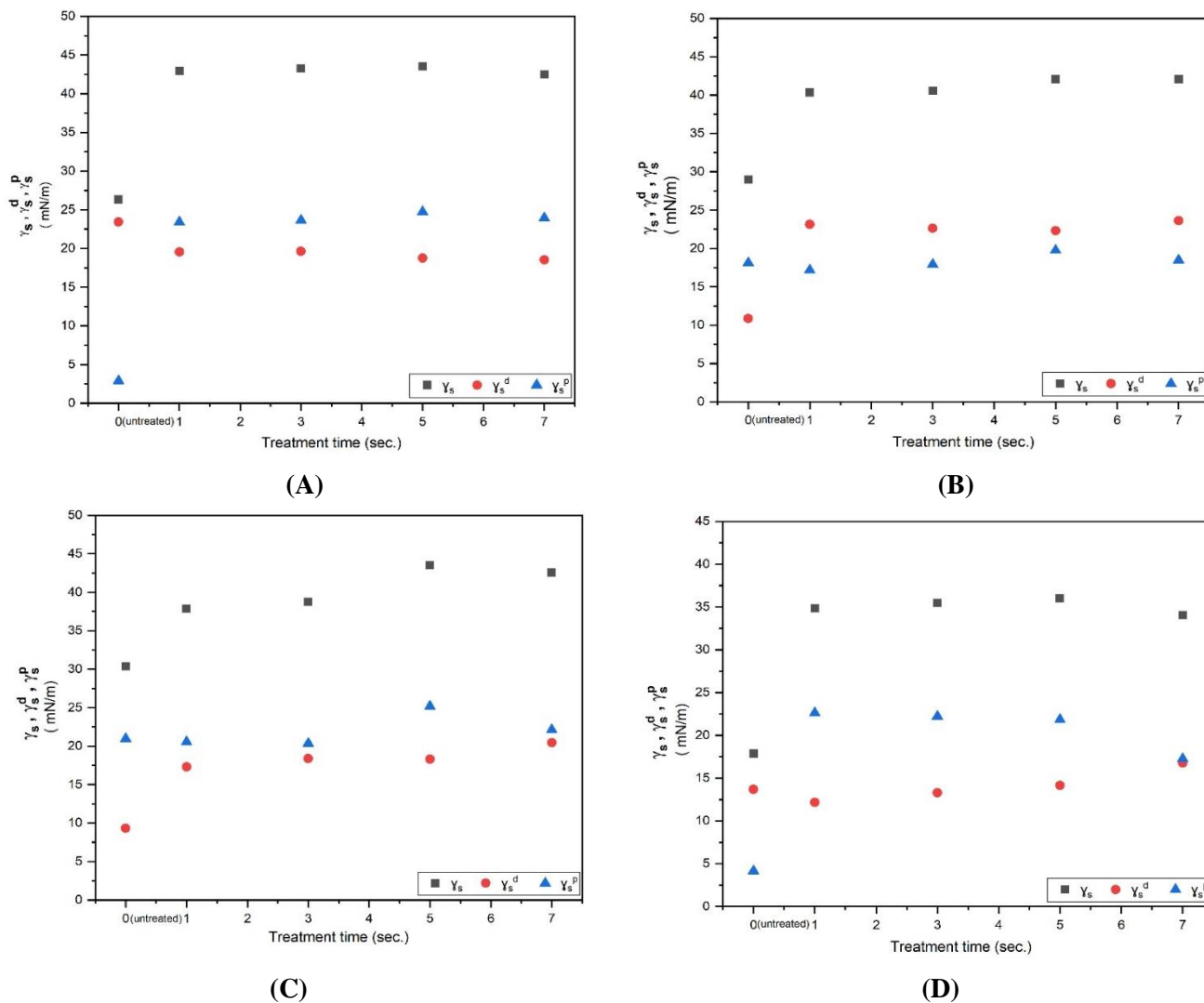


Figure 20 Surface free energy and its components (mN/m) of LDPE samples vs. corona-treatment time (sec.).
 (A): Competitor, (B): EC01-041, (C): EC01-049, (D):EC02

4.2.2 Surface morphology analysis

The change in the textural and morphological characteristics of the untreated and corona-treated LDPE surfaces were investigated by 2D SEM images measured at 20,000x magnification and resolution of 5.0 mm as shown in Figures 21-24. The untreated LDPE surfaces (Figures 21-24(A)) were characterized by smooth and very low surface roughness resulting from the manufacturing and polymerization processes. However, it was found that the surface roughness of unmodified LDPE EC01-049 (Figures 23 (A)) is slightly higher compared to the rest of the LDPE grades, this may be due to irregularities on the surface during the compression molding process by press

machine, or due to presence of polar covalent bonds within the structure. LDPE surfaces induced by the corona discharges (Figures 21-24 (B)) showed marked increase in surface roughness after 5s of plasma treatment, due to generation of polar groups as : hydroxyl (OH), carbonyl (C=O), and carboxyl acid (O=C-OH) as a results of ablation and functionalization processes on the amorphous phases of the LDPE surfaces [67]. It can be seen that the LDPE competitor surface has lower surface roughness compared with QAPCO LDPE as well as it contains unstable voids that can be removed easily with distilled water or a suitable solution as a result of oxidation after surface treatment by corona discharge.

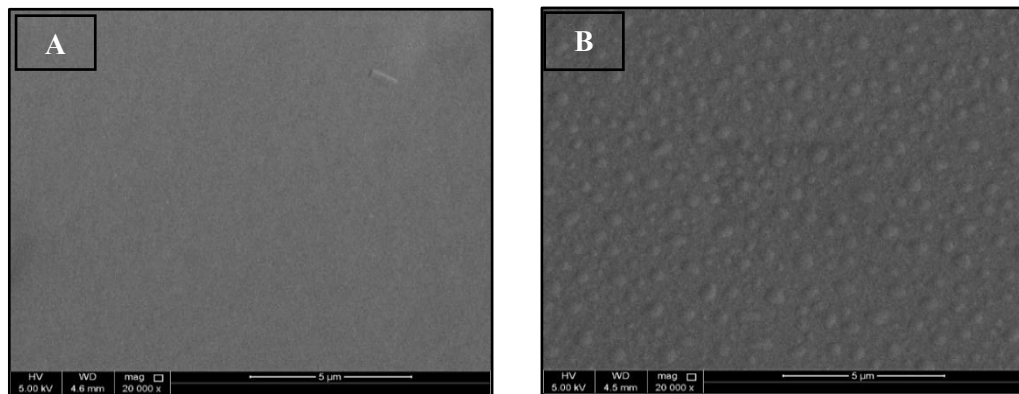


Figure 21 SEM images of LDPE Competitor surfaces : (A) untreated , (B) corona - treated (t=5s)

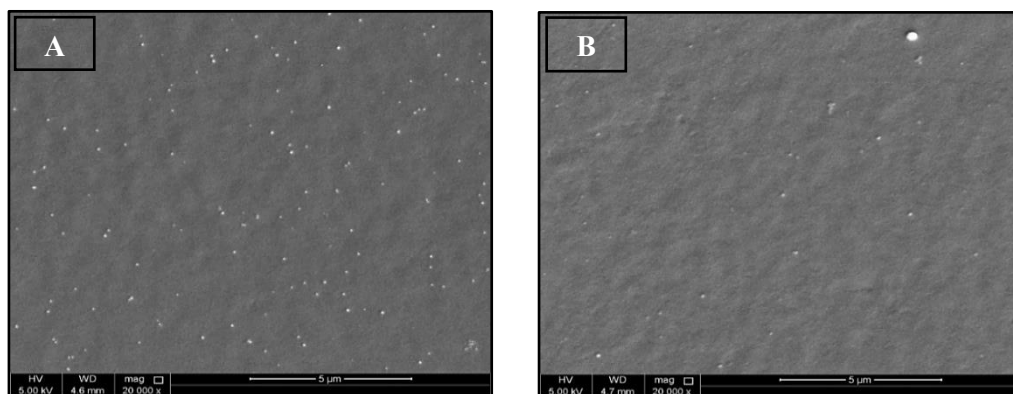


Figure 22 SEM images of LDPE EC01-041 surfaces : (A) untreated, (B) corona - treated (t=5s)

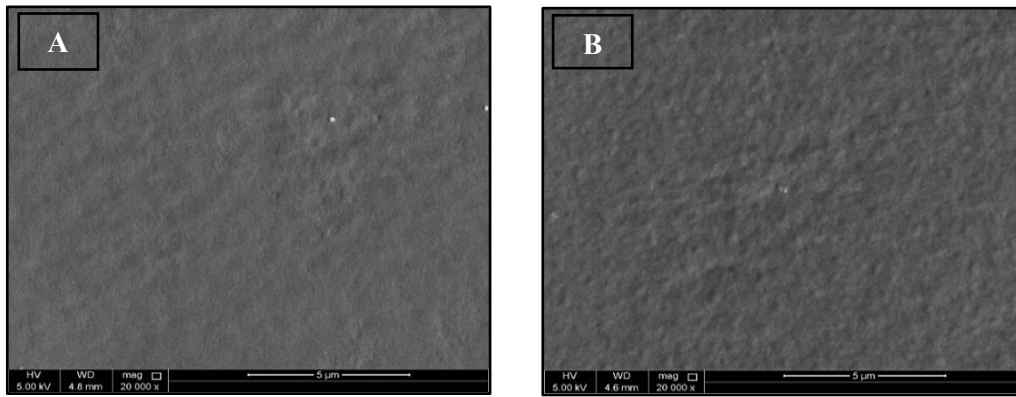


Figure 23 SEM images of LDPE EC01-049 surfaces : (A) untreated, (B) corona - treated (t=5s)

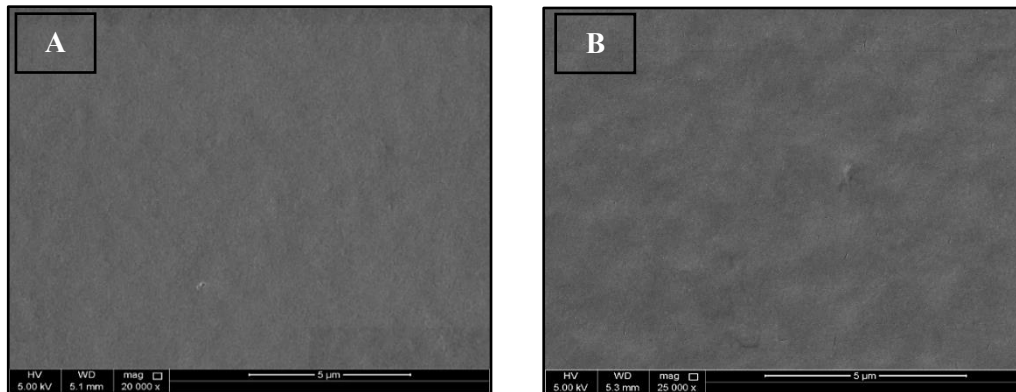


Figure 24 SEM images of LDPE EC02 surfaces: (A) untreated, (B) corona - treated (t=5s)

4.2.3 Surface compositions evaluation

The changes in the chemical compositions of the untreated and corona-treated LDPE surfaces were analyzed using Fourier-transform infrared spectroscopy (FTIR) in the range of 4000 cm^{-1} to 500 cm^{-1} wavelength as shown in Figure 25. Generally, FTIR spectrum of untreated LDPE is characterized by characteristic absorption peaks which coincide well with the relevant published literature, such as: out of phase and in-phase rock of the $-\text{CH}_2-$ at 720 cm^{-1} and 731 cm^{-1} , weak asymmetric bending vibration of carbon-hydrogen bond (C-H) along the vertical axis (b-axis) of the LDPE chain at 1478 cm^{-1} , asymmetric bending vibration of the CH_3 groups along the horizontal axis (a-axis bend) at 1463 cm^{-1} , as well as symmetric and asymmetric stretching vibrational bands that represent methylene group (CH_2) at 2848 cm^{-1} and 2916 cm^{-1} , respectively [90]. The surface modification due to the corona discharge led to show new absorbance bands in the LDPE infrared spectrum at 1750 cm^{-1} and 1110 cm^{-1} associated with stretching

vibrations of ester groups C=O (-COOH) and -O- respectively. Moreover, the hydroxyl functional group (-OH) was represented by a less intense and broad absorption peak between 3500 cm^{-1} and 3180 cm^{-1} . This can be attributed to the emergence of oxygen-containing functional groups on the modified surfaces. In addition, it was observed that the intensities of the functional groups absorption peaks were lower for LDPE competitor in comparison to the other LDPE grades. This is due higher content of carbon-carbon bonds on the surface as demonstrated by XPS analysis.

X-ray photoelectron spectroscopy (XPS) provides quantitative information about the elemental composition of the untreated and treated LDPE surfaces as illustrated in Figure 26 and Table 5. A significant increase in the oxygen content was observed after 1 second of surface treatment for all LDPE grades, from 2.15% to 11.74%, from 8.13% to 10.32%, from 8.62% to 11.33% , and from 4.38% to 4.54% for untreated and treated competitor , EC01-041, EC01-049, EC02 LDPE specimens respectively, due to incorporation of oxygen-containing functional radicals onto the corona-treated surfaces, as results of surface oxidation and activation. However, XPS spectrum showed relatively high atomic content of oxygen in the LDPE EC01 pristine structures. This may be related to the additives used during manufacturing. Moreover, unremarkable changes in the nitrogen atomic content (increased by 11% as maximum) were observed after 1s of surface treatment with corona discharge, due to weakly participate of nitrogen-associated functional groups (-C-N-) in the surface activation and modification processes. In contrast, a decrease in C-C content was observed in the treated-surfaces as follows, from 97.93% to 88.04% for untreated and treated LDPE competitor surfaces, 91.64% to 89.36% for untreated and treated LDPE EC01-041 surfaces, 91.20% to 88.47% for untreated and treated LDPE EC01-049, and from 93.46% to 93.37% for untreated and treated LDPE EC02. This could be explained due

to the extraction of surface carbon atoms and replacement them with the oxygen-containing polar species as result of functionalization and oxidation reactions.

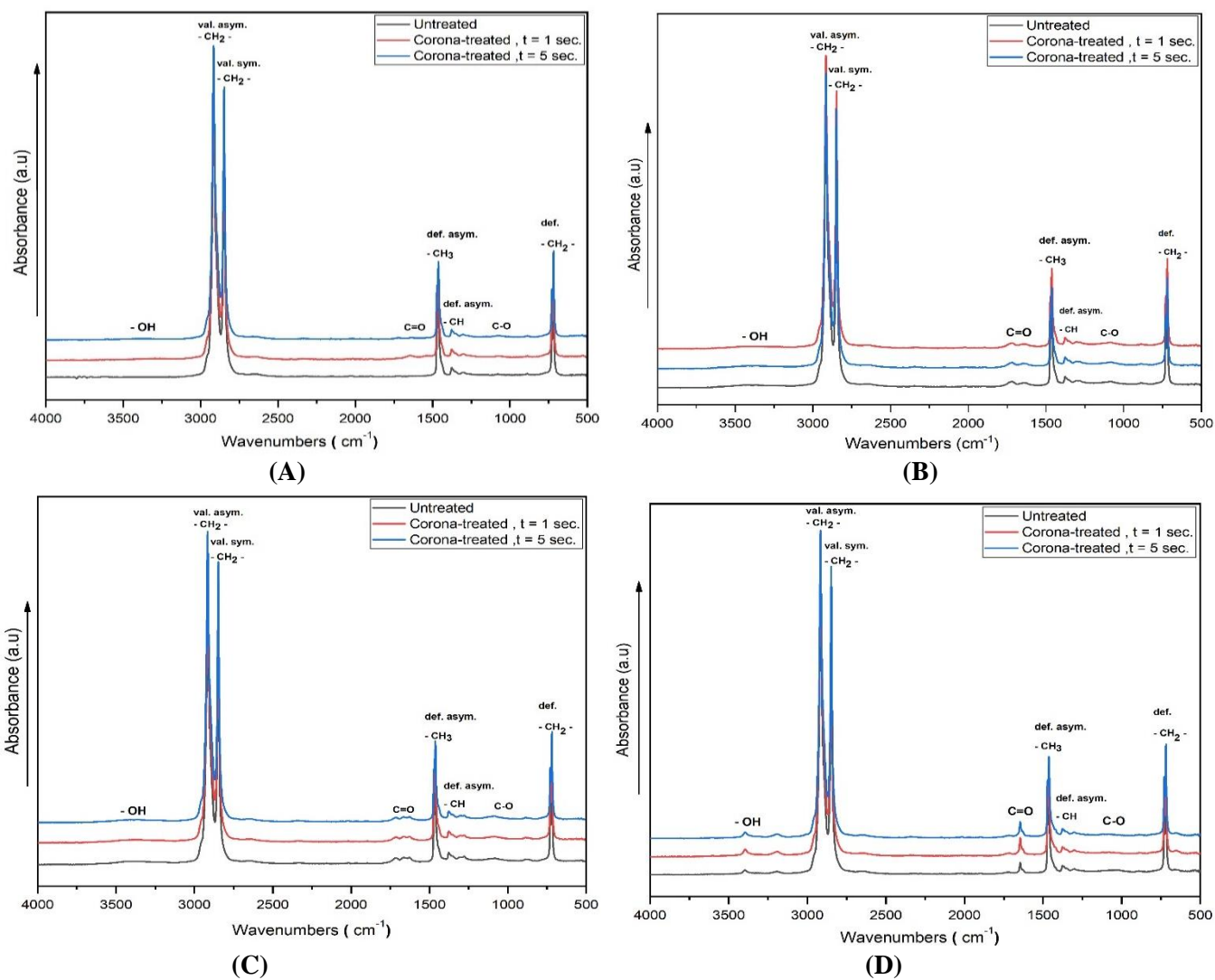


Figure 25 FTIR spectra of untreated and surface-treated LDPE grades.

(A): Competitor, (B): EC01-041, (C): EC01-049, (D):EC02

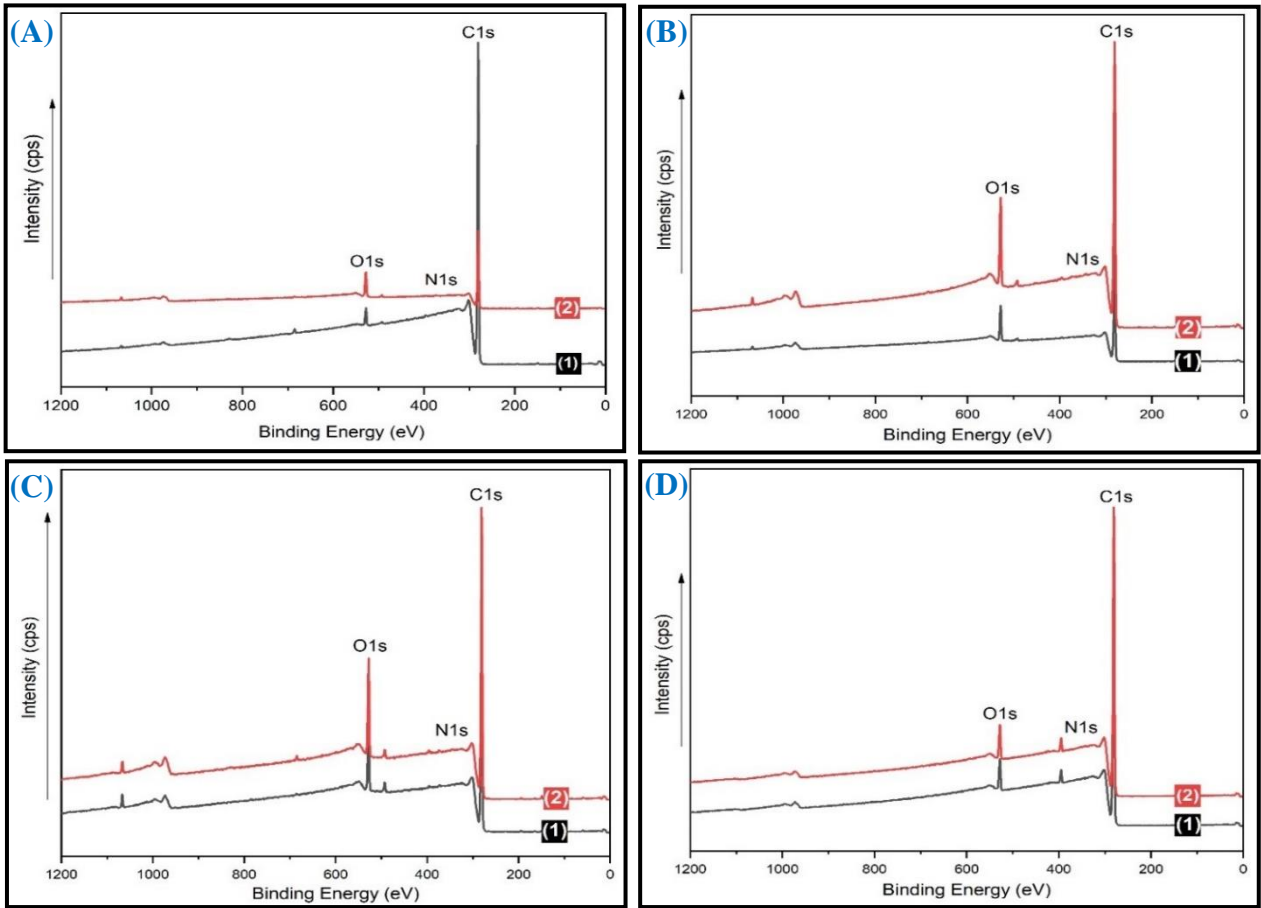


Figure 26 XPS spectra of LDPE grades : untreated (1) and 1 sec. corona-treated (2)
 (A): competitor, (B) : EC01-041,(C) : EC01-049,and (D) : EC02

Table 5 Elemental composition of untreated and corona-treated LDPE grades from XPS observations

LDPE Code	Element	Atomic Conc. (%)	
		Untreated (1)	Corona-Treated (2)
Competitor	C 1s	97.73	88.04
	N 1s	0.11	0.23
	O 1s	2.15	11.74
EC01-041	C 1s	91.64	89.36
	N 1s	0.24	0.32
	O 1s	8.13	10.32
EC01-049	C 1s	91.2	88.47
	N 1s	0.18	0.2
	O 1s	8.62	11.33
EC02	C 1s	93.48	93.37
	N 1s	2.14	2.09
	O 1s	4.38	4.54

4.2.4 Adhesive strength measurements

The increase of wettability of LDPE foils because of surface modification *via* corona discharge, resulted in an increase of adhesion strength (peel resistance – peel force per width) of corona-treated LDPE to Al foils, as evidenced in Figure 27. It must be noted in advance that high resistance means better adhesion between the laminate components. As can be seen, the peel resistance of LDPE/Al joints were examined with respect of variation in the corona radiation dosages $t = 0$ s (untreated), 3s, 5s, and 7s. The peel resistance of the pristine (untreated) LDPE/Al adhesion joints were nearly zero due to the hydrophobic nature and low wettability of untreated LDPE surfaces. Then, it was noticed the peel resistance of LDPE/Al laminates increased with longer time of surface treatment, as a result of higher surface roughness. In addition, the peel resistance of LDPE EC02 had recorded the lowest values for all treatment times

compared to the rest of LDPE grades, this may be due to the high carbon content even after surface treatment as proven by XPS analysis, as well as the low surface roughness demonstrated by SEM images.

The work of adhesion (W_{12}) for the LDPE/Al adhesive joints were calculated *via* contact angle measurements. It was found that W_{12} values give the similar behavior as the peel resistance for all conditions used. The reason for the low values of W_{12} is peeling of LDPE / Al adhesion joint were performed at extremely slowly crosshead speed compared with the peel resistance measured at a crosshead speed of 10 mm/min. However, it can be seen that the highest W_{12} were achieved after 5s of surface treatment *via* corona discharge due the highest values of surface polarity were observed at this treatment time.

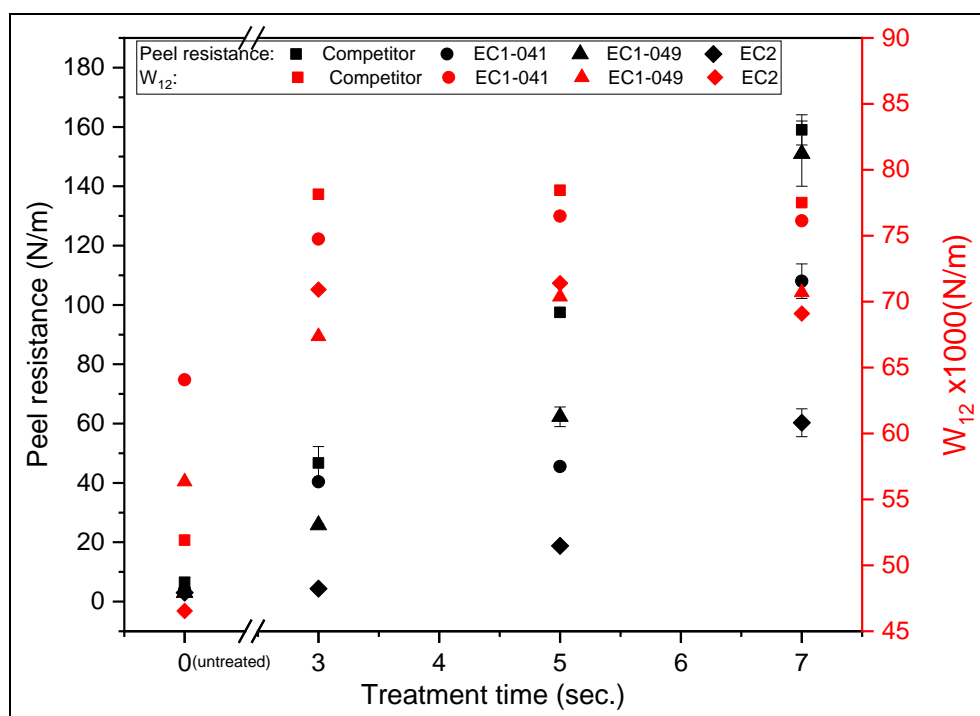


Figure 27 peel resistance, work of adhesion of LDPE/Al laminates as a function of corona treatment time of LDPE surfaces

4.3 Chemical modification of LDPE surfaces by free radical grafting with polyethylene glycol derivatives (PEG/PEO) in combination with corona discharge

Chemical modification based on grafting process of different concentrations of PEG/PEO containing aqueous solutions was applied immediately after the corona treatment. This combination of the two methods of surface treatment was tested on one LDPE grade, which is LDPE EC01-049 surfaces due to exhibit higher wettability as well as higher peel resistance to Al in compare with the rest of QAPCO LDPE grades. In addition to the above, uniform time (5s) was used for surface treatment using corona discharge, because at this treatment time, the maximum wettability and polarity of the corona-treated LDPE surfaces were achieved.

4.3.1 Grafting efficiency (% GE) calculation

Figure 28 represents the change in the grafting efficiency (%GE) of PEG/PEO grafted and corona-treated PEG/PEO grafted LDPE surfaces. It has been proven that surface treatment with corona electrical discharge contributes to increase %GE of PEG/PEO chains grafting onto LDPE surfaces. This can be interpreted as formation of functional radicals or reactive sites on the plasma-activated surface, these active sites (radicals) can later react with PEG/PEO chains that are introduced into the surface, which leads to increase the mass of the modified specimen, and thus increasing %GE. In other words, surface modification by combination of two different methods: plasma activation and conventional chemistry increases the grafting of the monomer chains into the treated LDPE surfaces [21]. However, most probably grafting mechanism can be caused by an esterification process [78] as the result of interactions between the incorporated carboxylic groups in LDPE and hydroxyl groups of PEG/PEO [75] as was confirmed by FTIR measurements. It was noted that GE% increased with increasing the PEG/PEO monomer concentration in the aqueous solution, due to formation of more

incorporation of reactive carbonyl groups (C=O) generated from PEG/PEO chains onto LDPE surfaces. Moreover, the highest %GE was achieved for PEO (300,000M) - g-LDPE at 5.0 wt.% concentration aqueous solution preceded by 5s surface treatment with corona discharge radiation, with an increase from 0.38 wt.% to 0.60 wt.% for untreated and plasma-treated LDPE surfaces, respectively. This is explained by PEO (300,000M) have ultrahigh molecular weights that creates a thick coating layer on the LDPE surface in comparison to the rest of the PEG used.

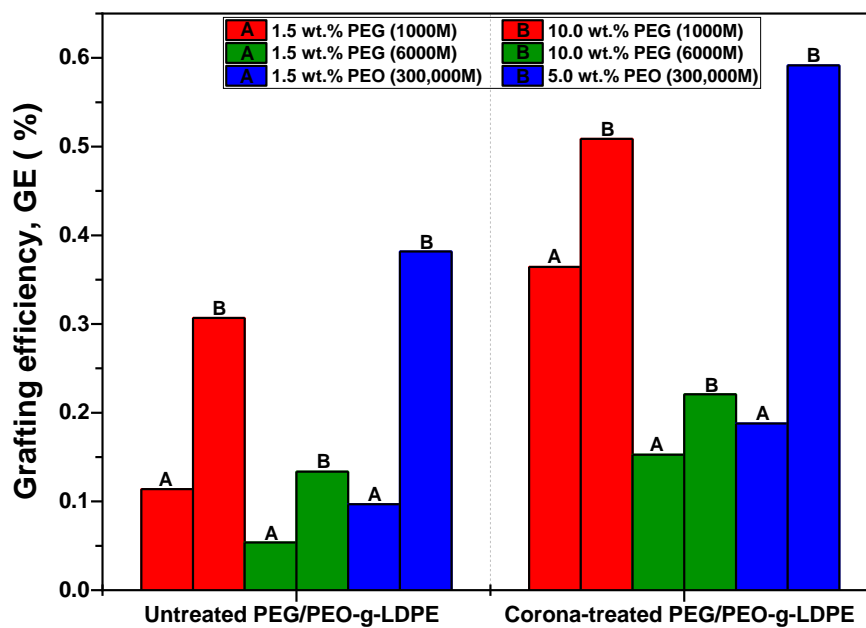


Figure 28 influence of surface treatment by corona discharge on GE (%) of PEG/PEO-g-LDPE surfaces

4.3.2 Surface wettability analysis

Figures (29-31) represents the wettability behavior of PEG/PEO-g-LDPE specimens with and without the surface treatment using corona discharge according to contact angle measurements. As can be seen, untreated PEG/PEO-g-LDPE surfaces presented slight reduction in contact angles in comparison with pristine (untreated) LDPE (e.g. water contact angle :72.33°), because of hydrophilic properties of the PEG/PEO molecules themselves [91]. In addition, the effect of surface treatment by corona discharge was studied on PEG/PEO-g-LDPE surfaces, whereas it was observed

dramatic decrease in the contact angle values for all the modified LDPE after plasma treatment, as a result of effective surface oxidation and functionalization. Furthermore, it was revealed that as the concentration of PEG/PEO grafted onto the LDPE surface increased the contact angle became higher for the same molecular weight, due to enrich the modified surface with PEG/PEO deposited as thin coating layer on the surface may reduce the surface interaction between wetting liquid and the exposed surface. However, it was found that the drop in the contact angle values for all the untreated and corona-activated PEG-g-LDPE surfaces were no more than 15 degrees at maximum compared to untreated LDPE (see Figure 19C), because PEG monomer structure consists of two hydrophilic hydroxyl groups on both sides of the chain covalently bonded to multiple carbon atoms linked together [75]. However, 10.0% PEG-g-LDPE (6,000M) films showed the greatest drop in the surface contact angle values after 5 sec. of surface treatment with corona discharge, from 69.11° to 61.46° for water, from 62.50° to 54.02° for formamide, and from 60.23° to 52.94° for ethylene glycol.

Figure 32 displays the change in the surface free energy and the corresponding polar and dispersive contributions of the and unmodified and corona-activated PEG/PEO-g-LDPE specimens. It was confirmed that surface modification *via* radical grafting with PEG/PEO- based initiator in conjunction with corona radiation contributed to improve the wettability properties of LDPE surfaces, as increase in both the surface energies and polarities were observed for all PEG/PEO used. This is due to introduction of characteristic polar functional groups, such as C=O, -OH, COOH, COO-, C-O-C, to the substrate surface. Thus, it was confirmed that surface modification of LDPE *via* plasma-initiated grafting of PEG/PEO contributed to an improve the wettability properties of LDPE surfaces, as an increase in both the surface energies and polarities were observed for all PEG/PEO used with estimated percentages of 31.3% and 63.0%,

respectively at the minimum compared with untreated LDPE. However, LDPE surfaces grafted with PEG/PEO showed close values of surface energy and its components which indicated that the molecular weight of grafted PEG/PEO slightly influence on the surface hydrophilicity.

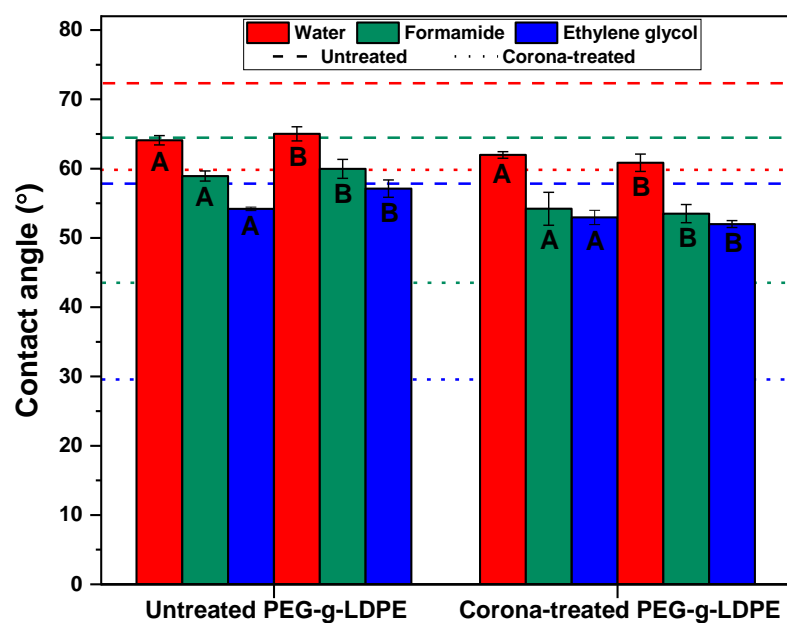


Figure 29 Contact angle of untreated and plasma -treated PEG (1,000M)-g-LDPE films: (A) 1.5 wt.% (B) 10.0 wt.%

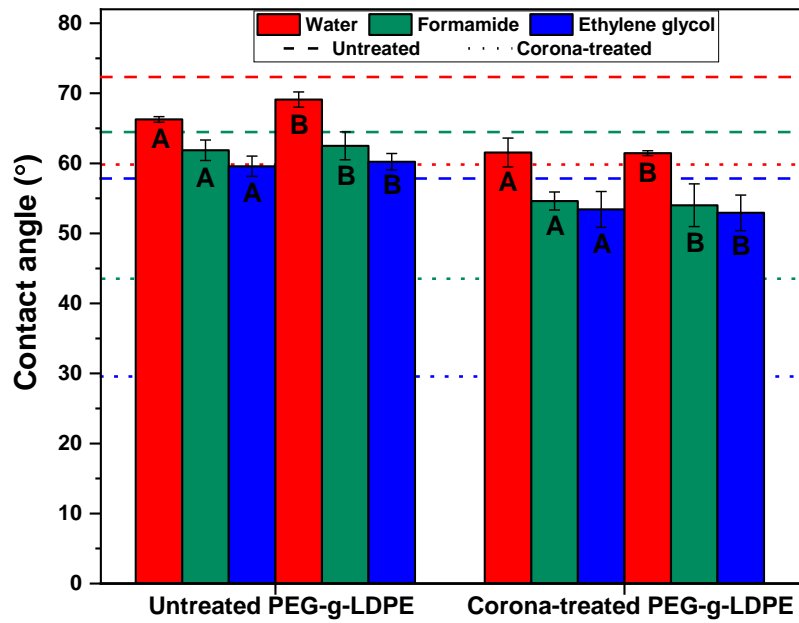


Figure 30 Contact angle of untreated and plasma -treated PEG (6,000M)-g-LDPE films: (A) 1.5 wt.% (B) 10.0 wt.%

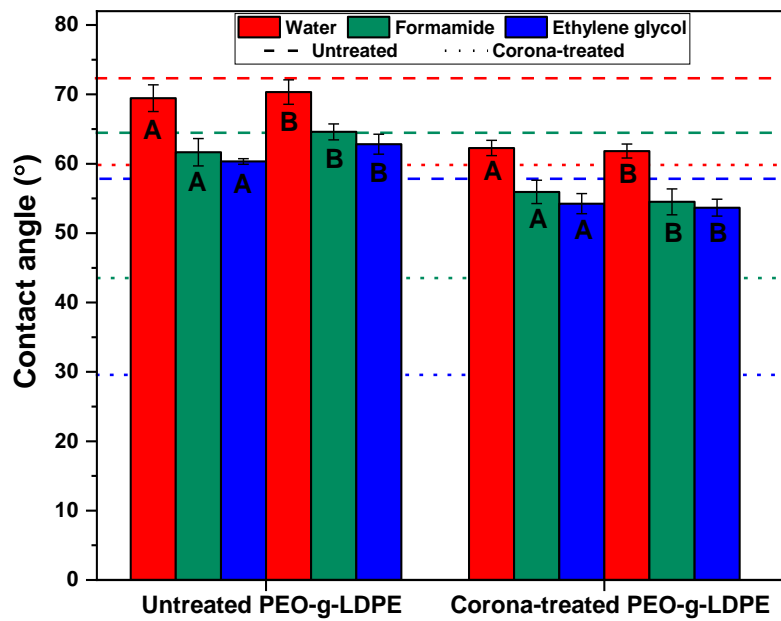


Figure 31 Contact angle of untreated and plasma -treated PEO (300,000M)-g-LDPE films: (A) 1.5 wt.% (B) 5.0 wt.%

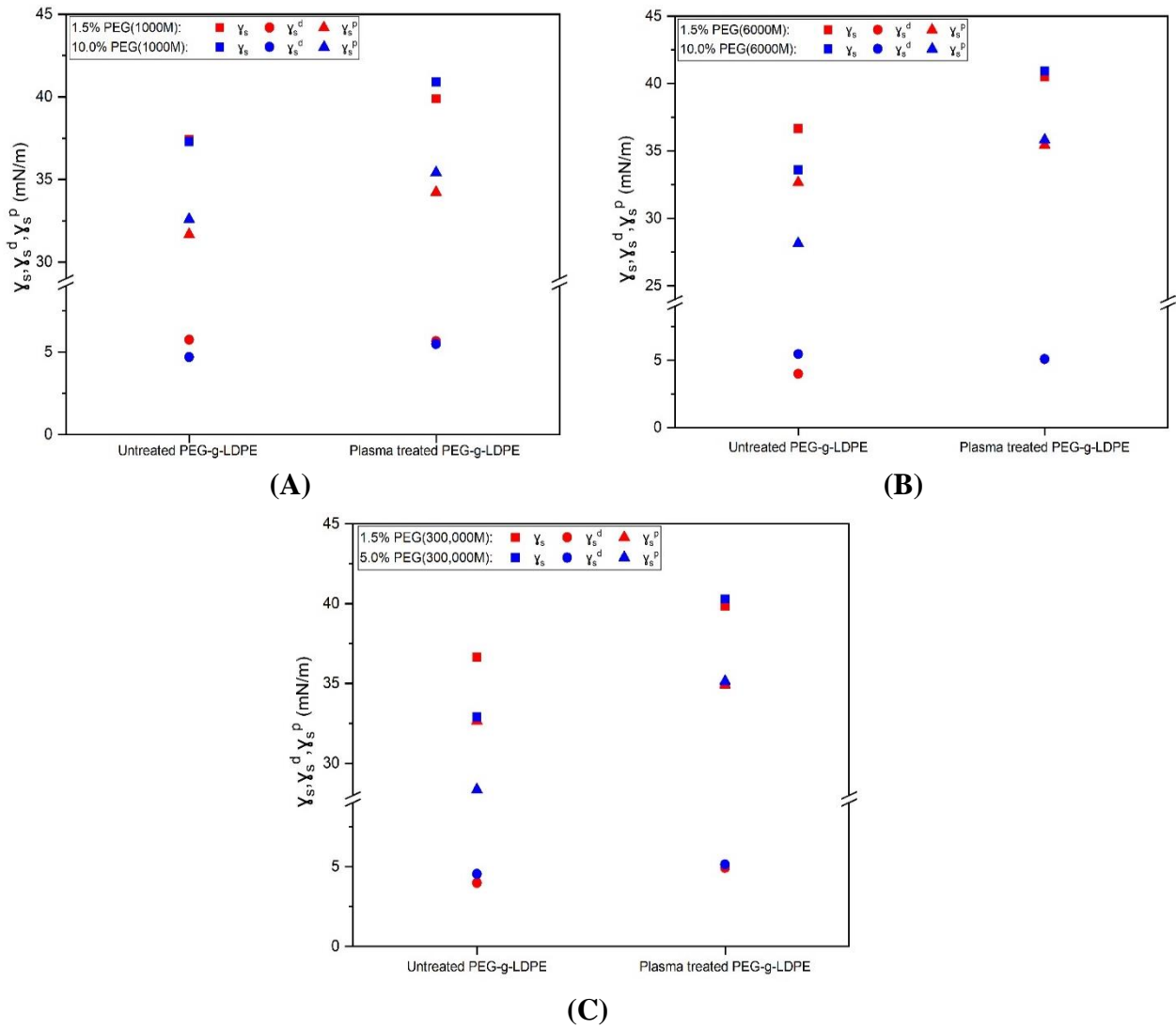


Figure 32 Surface energy (γ_s) and its derivatives: polarity (γ_s^p), and dispersion (γ_s^d) of untreated and corona treated PEG/PEO-g-LDPE surfaces

(A) 1000M PEG, (B) 6000M PEG, (C) 300,000M PEO

4.3.3 Surface morphology analysis

The surface morphology of untreated and corona treated-PEG/PEO grafted LDPE specimens was analyzed by scanning electron microscopy (SEM) as are shown in Figures 33-35 SEM images showed that 5 sec corona treated PEG/PEO-g-LDPE films Figures 33-35 (B,D) have non-considerable increase in surface roughness compared to untreated LDPE surface (Figure 23(A)), while less rough compared to corona-treated LDPE surface (Figure 23(B)) due to formation of a compact PEG/PEO layer in the amorphous phase of LDPE, which changes the surface texture.

After grafting; SEM images of untreated PEG/PEO-g-LDPE surfaces (Figures 33-35 (A,C)) revealed a uniform smooth textures with a low levels of surface roughness due to the relatively high grafting density of PEG/PEO on the surface [79] In contrast, it was observed a significant increase in surface roughness predominantly in the amorphous phase on the plasma-exposed PEG/PEO grafted LDPE surfaces, as influence of oxidation and etching processes because of corona discharge. Furthermore, it was found the formation of porous and loose granules on the corona-treated

PEG/PEO-g-LDPE surface as a result to agglomeration of PEG/PEO particles on the LDPE surface ((Figures 33-35 (B,D)).

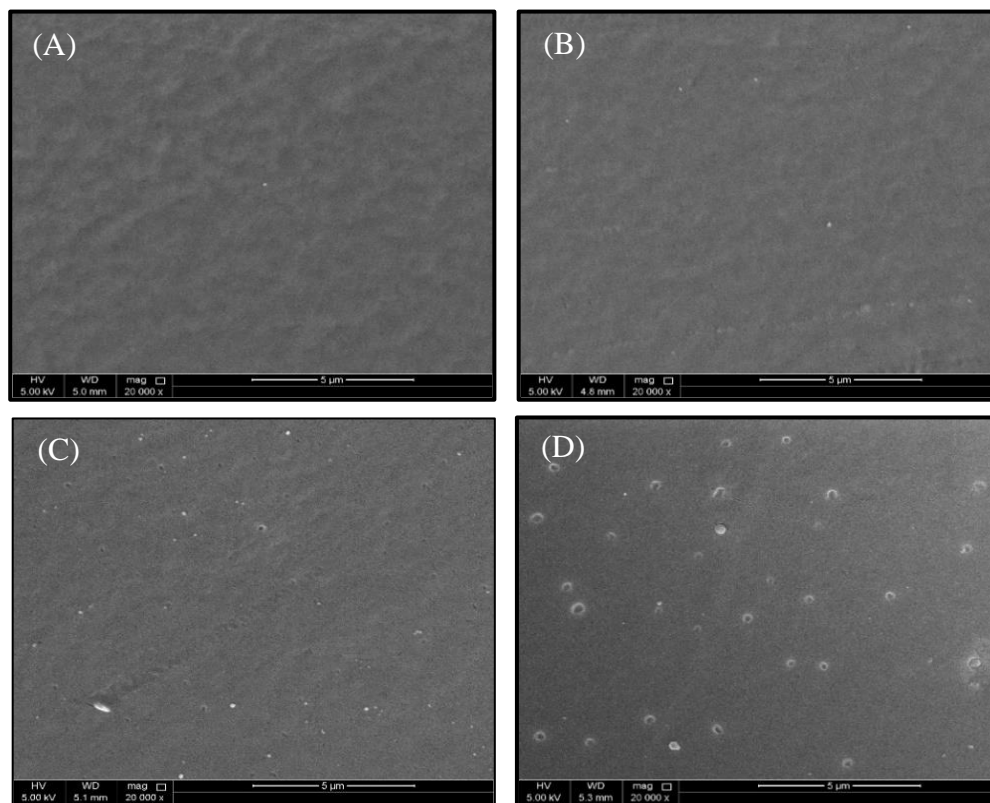


Figure 33 SEM micrographs of PEG-g-LDPE (1,000M) water solution

(A) untreated 1.5 wt.% PEG- g-LDPE (B) corona-treated (t=5s) 1.5 wt.% PEG- g-LDPE
(C) untreated 10.0 wt.% PEG- g-LDPE (D) corona-treated (t=5s) 10.0 wt.% PEG- g-LDPE

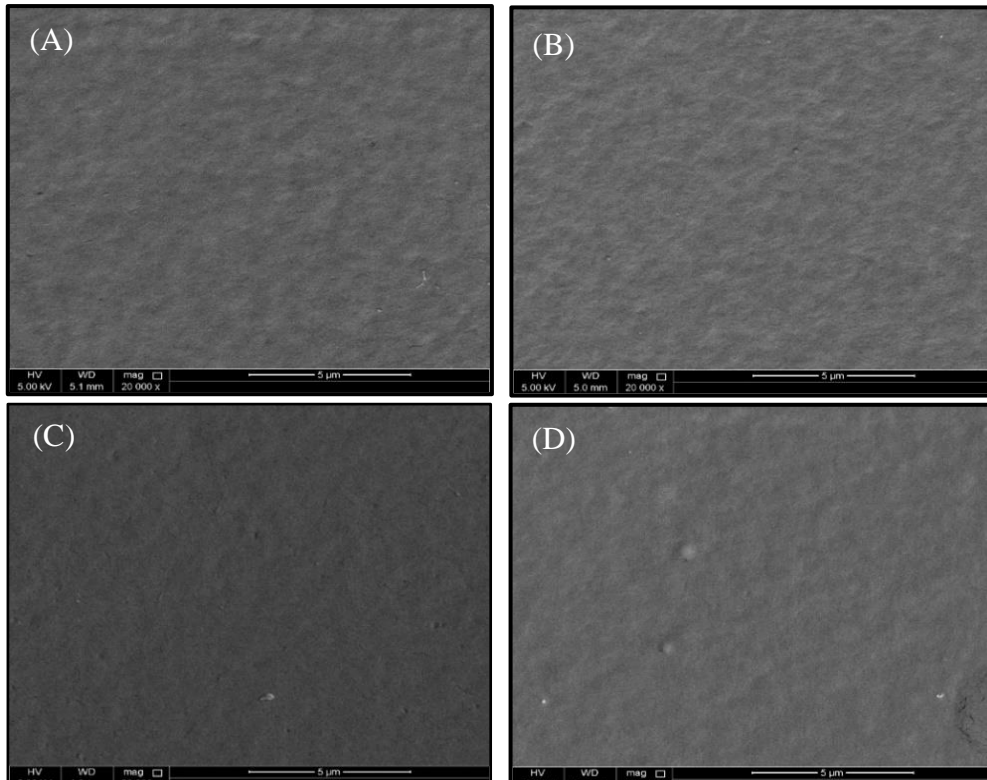


Figure 34 SEM micrographs of PEG-g-LDPE (6,000M) water solution

(A) untreated 1.5 wt.% PEG-g-LDPE (B) corona-treated (t=5s) 1.5 wt.% PEG-g-LDPE
 (C) untreated 10.0 wt.% PEG-g-LDPE (D) corona-treated (t=5s) 10.0 wt.% PEG-g-LDPE

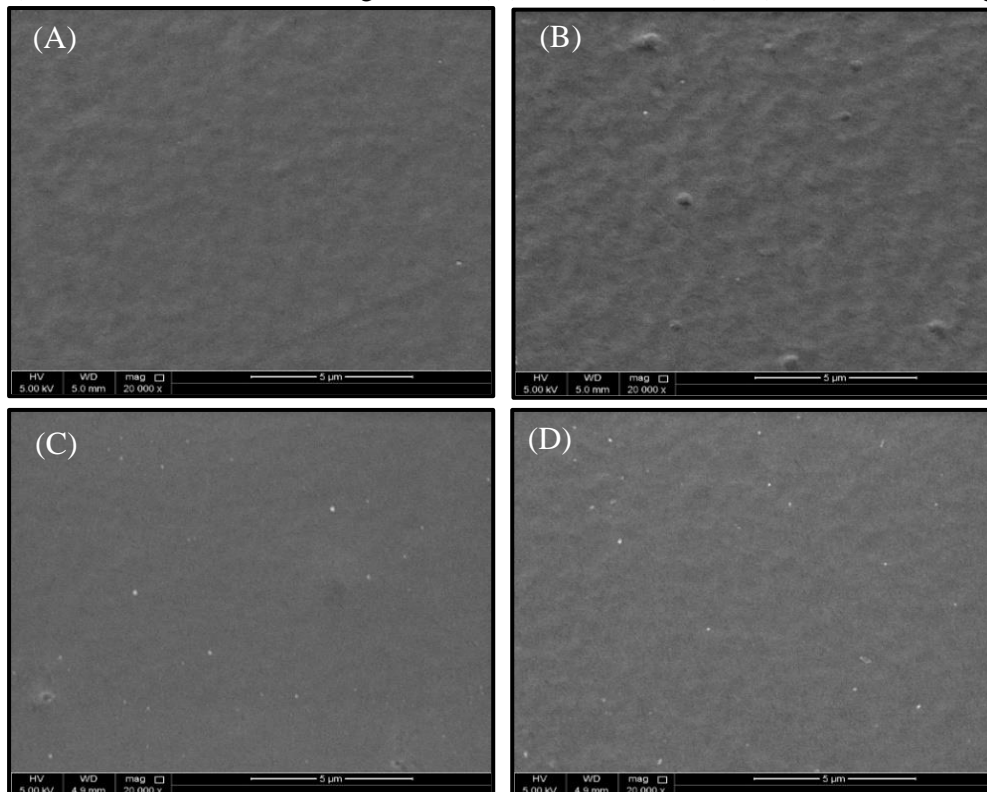


Figure 35 SEM micrographs of PEO-g-LDPE (300,000M) water solution

(a) untreated 1.5 wt.% PEO-g-LDPE (b) corona-treated (t=5s) 1.5 wt.% PEO-g-LDPE
 (c) untreated 10.0 wt.% PEO-g-LDPE (d) corona-treated (t=5s) 5.0 wt.% PEO-g-LDPE

The AFM measurements were performed in order to analyze detailed surface morphology/topography changes in the LDPE surface after plasma treatment and modification processes, as evidenced in Figures 36-39 to compare with the AFM images that represent untreated and 5 s corona-treated LDPE films (Figure (36)). The changes in the surface roughness were quantified by the surface roughness parameter (R_a). AFM images showed that the surface of the untreated LDPE is relatively smooth with low value of average roughness ($R_a = 3.37$ nm), as demonstrated in Figure (36(a)). Correspondingly, the surface treatment of the LDPE surface with 5s of corona discharge led to increase in the surface roughness ($R_a = 4.49$ nm) because of incorporation of oxygen containing functional groups on the treated surfaces associated with consecutive oxidation and functionalization reactions (Figure 36 (b)). In addition, it was noticed that surface roughness decreased after PEG/PEO grafting onto the LDPE surfaces (Figures 37-39) compared to corona-treated surfaces, due to a formation of PEG/PEO layer onto the LDPE surface, where PEG/PEO forms strong bonds between PEG/PEO radicals and surface carbon atoms by functionalization reaction. Furthermore, it was found increasing the concentration of the PEG/PEO based aqueous solution resulted less rough LDPE surface, due to high grafting density of PEG/PEO that leads to create a thick layer on the amorphous regions of LDPE surfaces. In addition, it was found that LDPE surfaces treated with PEG(6000M) had higher R_a values, confirming that these surfaces are characterized with high surface roughness and extremely good wettability properties. Moreover, it was observed that all LDPE films grafted by high concentrations of PEG/PEO had almost same surface roughness ($\approx R_a=3.6$ nm). This is indicative of the limited grafting of PEG/PEO onto LDPE surfaces as a result of surface degradation.

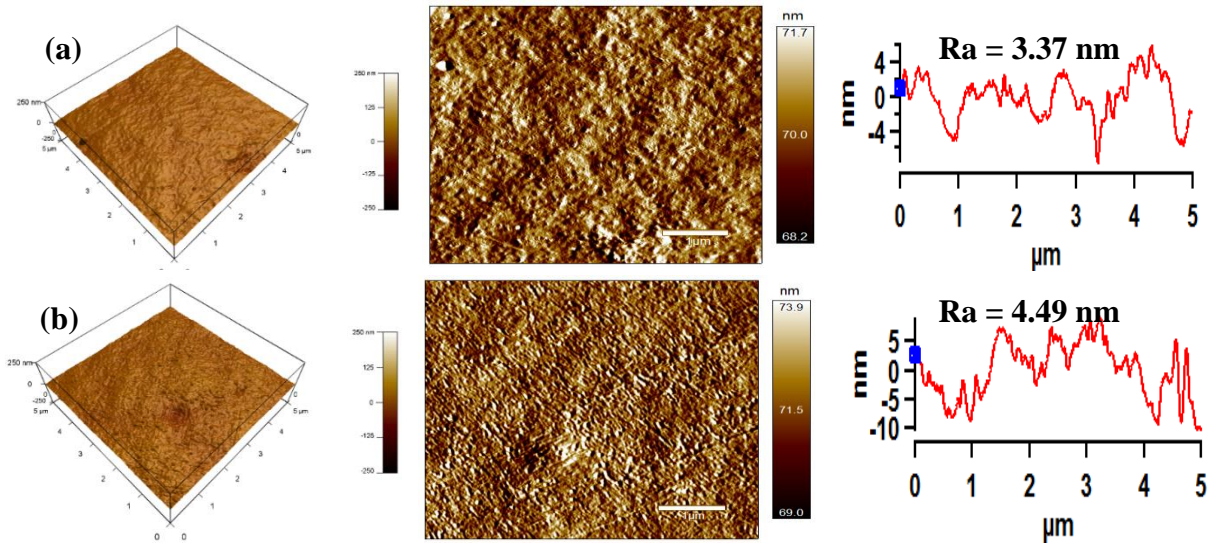


Figure 36 AFM images with Ra roughness parameter of (a) untreated (b) corona treated LDPE surfaces

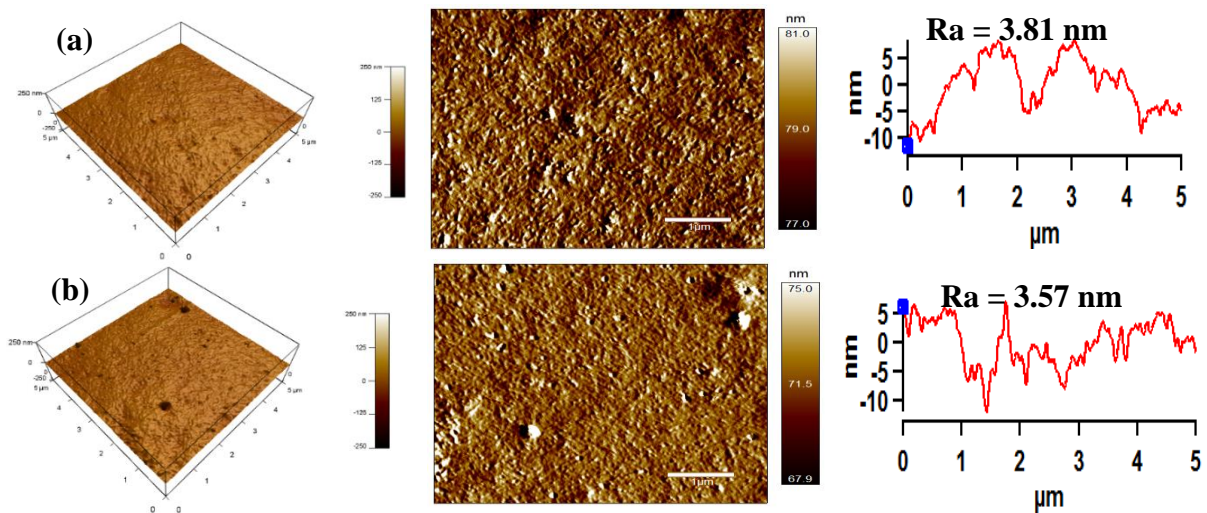


Figure 37 AFM morphological images and line scans of corona activated LDPE films which surface grafted by PEG (1000M) aq. solutions with concentration of (a) 1.5 wt.% , (b) 10.0 wt.%

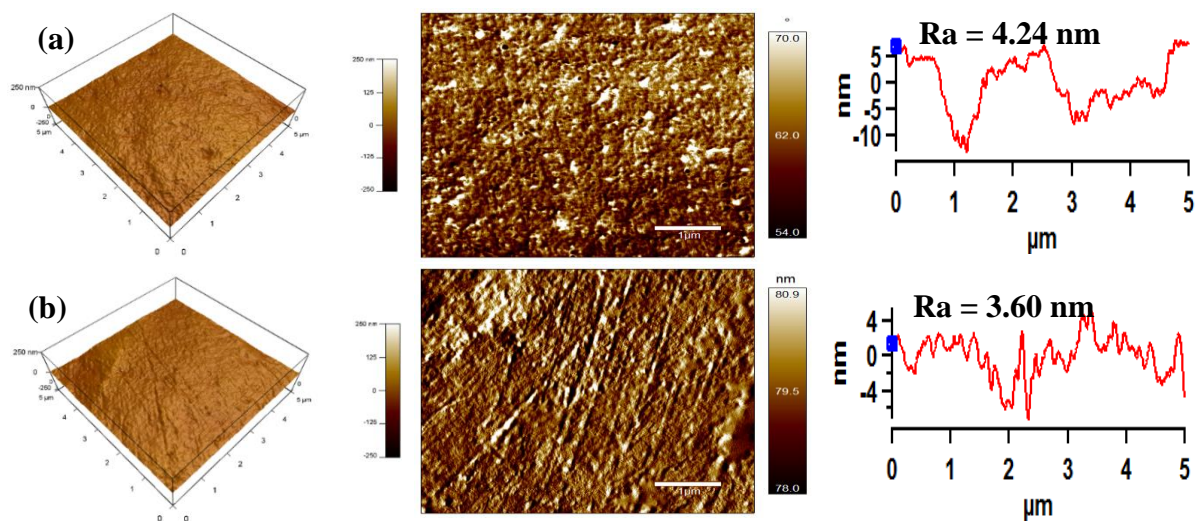


Figure 38 AFM morphological images and line scans of corona activated LDPE films which surface grafted by PEG (6000M) aq. solutions with concentration of (a) 1.5 wt.% , (b) 10.0 wt.%

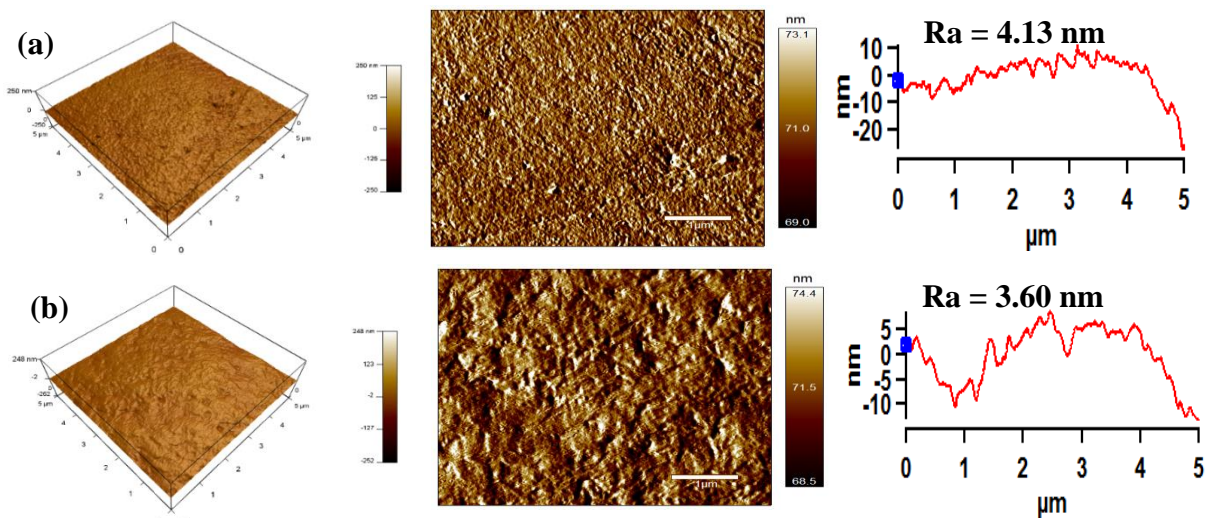


Figure 39 AFM morphological images and line scans of corona activated LDPE films which surface grafted by PEO (300,000M) aq. solutions with concentration of (a) 1.5 wt.% , (b) 5.0 wt.%

4.3.4 Chemical composition investigation

FTIR spectra was employed to investigate the change in the chemical compositions after grafting of PEG/PEO-g-LDPE films after surface activation with corona radiation (Figure 40). It was observed that FTIR spectrum of PEG/PEO-g-LDPE surfaces exhibited noticeable increase in the peak intensity corresponds to ether group (–O–) compared with only corona-treated LDPE samples, while the peak intensities of carbon-hydrogen bond (C-H) carboxyl group (C=O) both decreased. Moreover, the FTIR spectra clearly indicates the disappearance of the hydroxyl group COOH-associated absorption bands in the PEG/PEO-g-LDPE samples, which were utilized in the grafting process.

X-ray photoelectron spectroscopy (XPS) provides quantitative information about the elemental compositions of the treated PEG/PEO-g-LDPE surfaces as seen in Figure 41 and Table 6. As can be seen, there are two characteristic XPS peaks corresponding to the C1s and O 1s at binding energy values of 284.8 eV, and 532.8 eV, respectively. A

slightly increase in the oxygen content was observed after corona treatment, while at.% of O1s increased from 8.6% to 11.3% for untreated and corona-treated LDPE, respectively, due to enrich the surface with oxygen-containing functional groups. However, the presence of oxygen species in the untreated LDPE structure may be related to the processing additives. After PEG/PEO grafting onto LDPE surfaces *via* plasma treatment, it was found that the at.% of carbon element increased compared to untreated LDPE as results of PEG/PEO grafting. It was observed slightly increase at.% of O1s with increasing the molecular weight of grafted PEG/PEO chains due to incorporation of reactive carbonyl groups (C–O–C) generated from PEG/PEO chains onto corona-treated LDPE surfaces. Therefore, it was showed that at.% carbon elements decreased, due to the replacement of the surface carbon atoms with the oxygen functional groups. Furthermore, a decrease in the nitrogen content was observed on the LDPE surfaces with increasing the molecular weight of grafted PEG chains (>1,000), because PEG chains able to form a thin coating layer on the LDPE surface, which hinders the detection of the internal nitrogen element [79]. Moreover, XPS spectra showed presence of fluoride (F1s) of PEO-g-LDPE (300,000M) surfaces at 687 eV binding energy, because LDPE rinsed with distilled water several times to remove excessive PEO chains, thus probably some water molecules were still stuck on these surfaces.

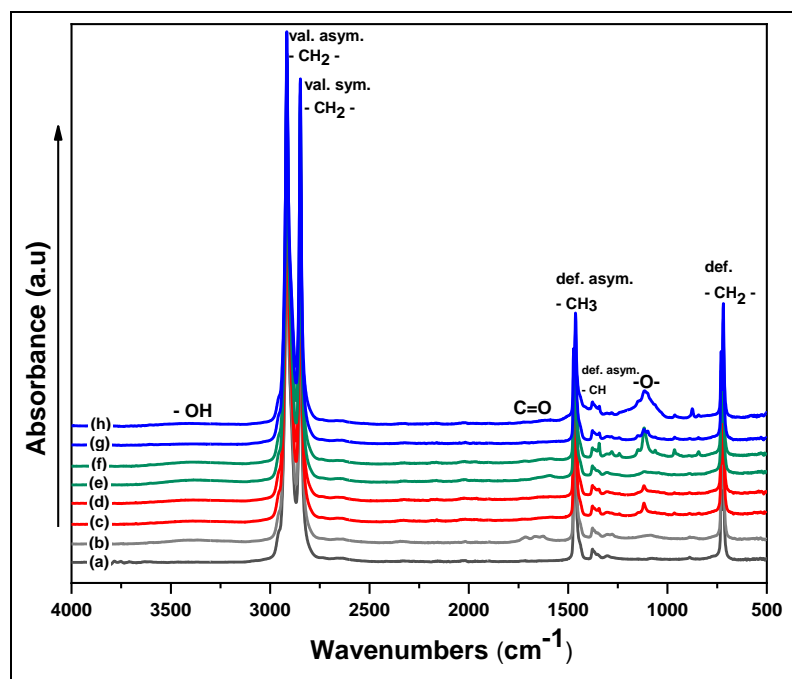


Figure 40 FTIR spectra of LDPE surfaces:

- (a) untreated, (b) corona-treated,
- (c) 1.5 wt.% PEG(1000M)-g-LDPE, (d) 10.0 wt.% PEG(1000M)-g-LDPE,
- (e) 1.5 wt.% PEG(6000M)-g-LDPE, (f) 10.0 wt.% PEG(6000M)-g-LDPE,
- (g) 1.5 wt.% PEO(300,000M)-g-LDPE, (h) 5.0 wt.% PEO(300,000M)-g-LDPE.

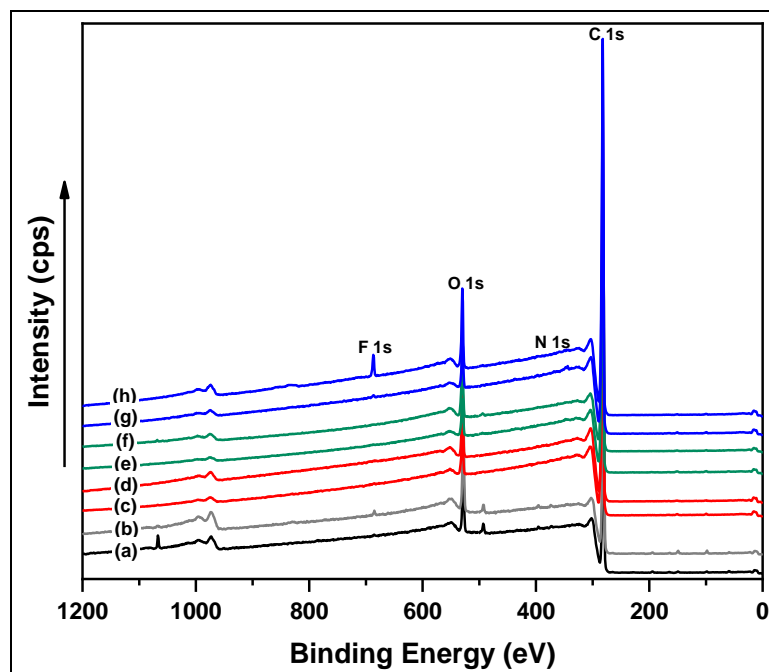


Figure 41 XPS spectra of LDPE surfaces

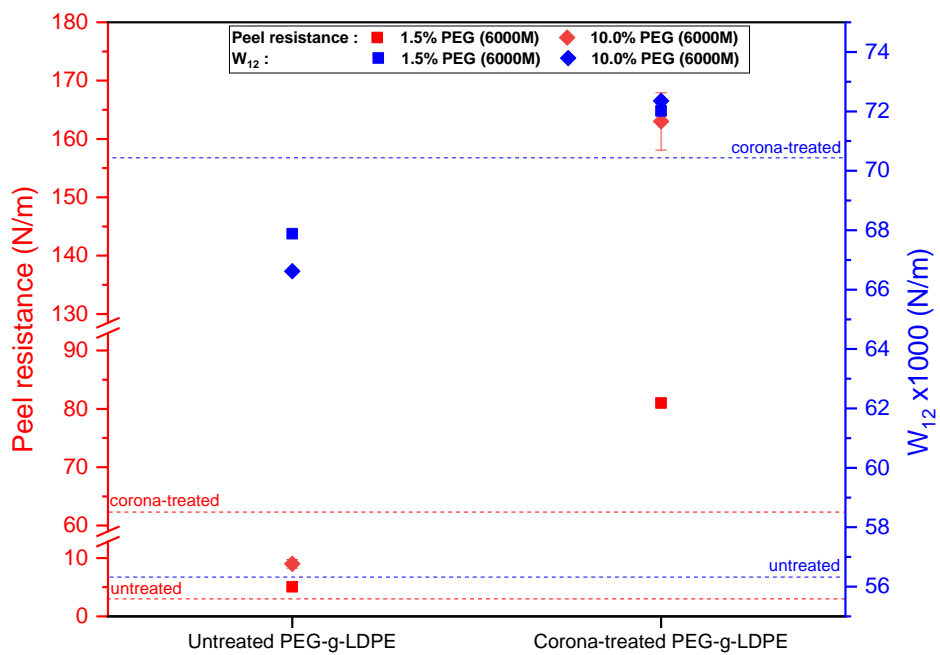
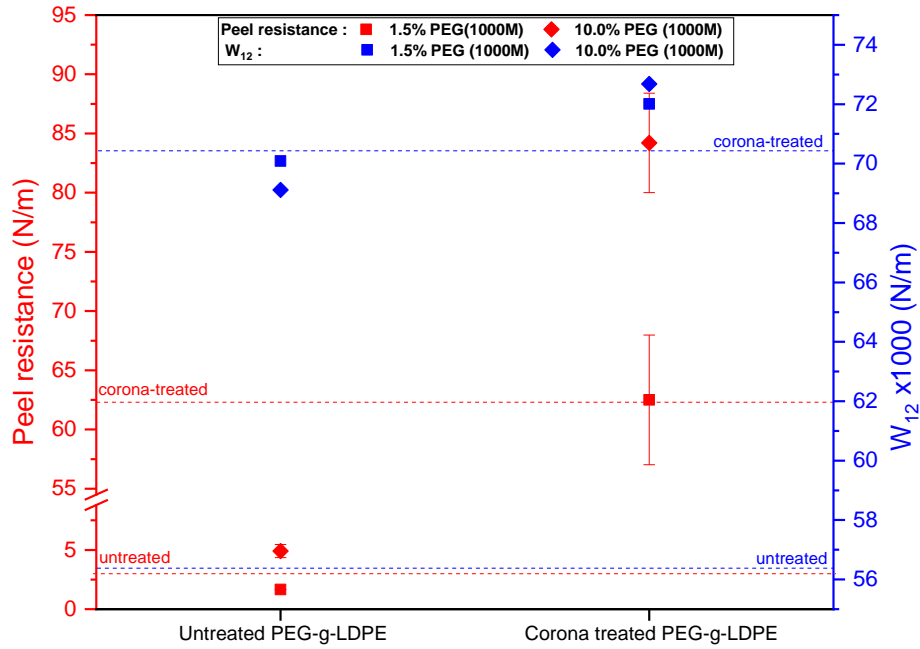
Table 6 elemental composition of LDPE surfaces by XPS analysis

Samples	Element, Atomic conc. (at. %)		
	C 1s	O 1s	N 1s
(a) Untreated-LDPE	91.2	8.62	0.18
(b) Corona-treated LDPE	88.47	11.33	0.20
(c) 1.5 wt.% PEG (1000M)-g-LDPE	95.18	4.64	0.17
(d) 10.0 wt.% PEG (1000M)-g-LDPE	93.61	6.08	0.31
(e) 1.5 wt.% PEG (6000M)-g-LDPE	95.25	4.51	0.00
(f) 10.0 wt.% PEG (6000M)-g-LDPE	92.33	7.52	0.04
(g) 1.5 wt.% PEO (300,000M)-g-LDPE	95.05	5.22	0.03
(h) 5.0 wt.% PEO (300,000M)-g-LDPE	90.59	9.17	0.00

4.3.5 Adhesive strength measurements

The adhesive properties of untreated and plasma treated PEG/PEO-g-LDPE films bonded into Al foils were investigated by peel test measurements, as well as work of adhesion calculations (Figure 42). It was observed that LDPE/Al adhesion joints associated with LDPE surfaces coated with PEG had slightly higher peel resistance compared with pristine LDPE (nearly 3 N/m), due to the fact that the PEG/PEO compounds have limited hydrophilic properties. However, the peel resistance of LDPE/Al laminates were significantly increased after modification LDPE surfaces with 5 sec. of corona discharge for all used PEG/PEO grafting. This increase in peel resistance is mainly due to enhanced wettability and increased the surface roughness as a result of surfaces oxidation and activation *via* corona radiation. In addition, the highest peeling resistance values were recorded at high concentrations of PEG/PEO aqueous solutions, which is consistent with the surface wettability results obtained from the contact angle measurements of PEG-g-LDPE surfaces. The maximum peel resistance (163.0 N/m) of LDPE/Al adhesive joint had measured at 10.0wt.% PEG (6000M)-g-LDPE surfaces, which suggested as the optimum value. In contrast, the corona-treated PEO (300,000M)-g-LDPE surfaces exhibited the lowest adhesion values compared to the rest of the PEG used. This might predict to formation of higher density of the PEO coating on the LDPE surfaces, which relatively reduced LDPE to be adhered to Al. On the other hand, the work of adhesion (W_{12}) for the PEG/PEO-g-LDPE/Al adhesive joints were determined by contact angle measurements. In general, it was found that all modified PEG/PEO-g-LDPE surfaces have higher values of W_{12} compared to untreated and corona-treated LDPE surfaces resulted from the improved wettability. However, it was concluded that corona-activated 10.0 wt.% PEG(6000M)-g-LDPE surface had higher W_{12} (71.36 N/m) compared to the rest of modified LDPE surfaces grafted by

PEG chains, because of the high polarity that was recorded for this surface. This corresponds to the peel resistance results.



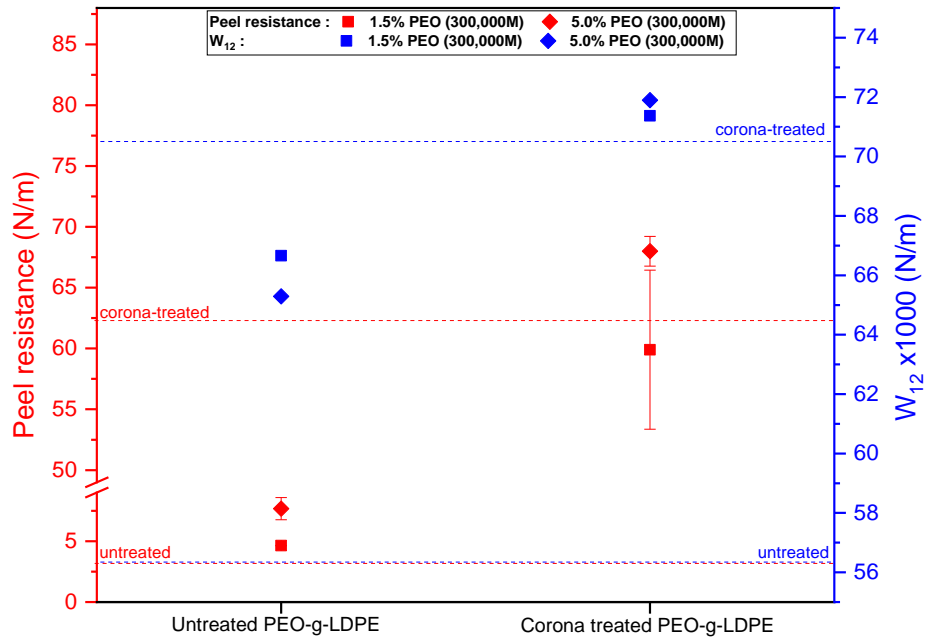


Figure 42 Effect of corona treatment on the peel resistance and work of adhesion of PEG/PEO-g-LDPE adhesive joint with Al.

CHAPTER 4: CONCLUSION

In this work, the surface characteristics of QAPCO Low-density polyethylene (LDPE) grades were successfully enhanced using two different potential techniques, which are: corona discharge based on ionization of air, and chemical modification *via* radical grafting of different molecular weight PEG/PEO chains onto LDPE surfaces. Both techniques contributed to improve the wettability and polarity of LDPE surfaces which were represented by contact angles measurements, increase the surface roughness, and change in surface morphology which were observed by topographical analyses, change in the chemistry of the modified surfaces due to introduction of the oxygen-containing polar functional groups onto the surfaces as confirmed by chemical composition spectroscopy instruments. Consequently, significant improvement in adhesion between LDPE and Al was achieved after surface modification and verified by the peel resistance test and work of adhesion calculations. Thus, the highest bond strength was achieved after five seconds of surface treatment of the LDPE surface with continuous ionization *via* corona discharge radiation, followed by radical grafting with 10 wt.% PEG (6000 M) aqueous solution, and it was approximately 163 N / m. Thus, it can be asserted that the peel resistance at the optimum condition increased by approximately 54 times and 2.6 times compared to the peel resistance of untreated and corona-treated LDPE surfaces, respectively.

CHAPTER 5: FUTURE WORK

It would be useful to follow these tasks in order to achieve better results about surface modification of QAPCO LDPE grades, and hence, to use them in the manufacture of Tetra Pak food containers.

- I. Investigate the differences in the microstructure of LDPE grades produced by QAPCO, according to degree of chain branching, degree of crystallinity, molecular weight distribution, and dynamic rheological parameters of PE melts using the appropriate characterization tools. Therefore, the relationship between the microstructure of LDPE and the change in the surface characteristics after surface modification, and thus the adhesion strength with Al will be studied.
- II. The optimal results of each performed test on PEG/PEO-g-LDPE EC01-049 will be selected to re-apply to the rest of the LDPE grades: competitor, EC01-041, and EC02, to verify that maybe LDPE grade gives same behavior. These tests include: grafting efficiency (GE) determination, surface wettability investigation based on contact angle measurement, adhesion strength of LDPE/Al laminate according to 90-degree peel test. Furthermore, same surface morphology and chemical compositions analyses will be employed for each LDPE grade at the same tested conditions .
- III. The optimum condition of PEG/PEO grafting will repeat on EC01-049 surface after treating both LDPE and Al with corona discharge in order to achieve expected higher adhesion to Al.
- IV. Use other compounds /polymers *via* radical grafting onto LDPE grades after surface treatment with corona discharge, with the aim of to achieve higher surface hydrophilicity and thus improve their adhesion with Al.

REFERENCES

1. Rabnawaz, M., et al., *A roadmap towards green packaging: the current status and future outlook for polyesters in the packaging industry*. Green Chemistry, 2017. **19**(20): p. 4737-4753.
2. Yang, F., et al., *Copolymerization of propylene with higher α -olefins by a Pyridylamidohafnium catalyst: An effective approach to polypropylene-based elastomer*. Polymers, 2020. **12**(1): p. 89.
3. Sharpe, P., *Making Plastics: From Monomer to Polymer*. Chemical Engineering Progress, 2015. **111**: p. 24-29.
4. Amin, S. and M. Amin, *Thermoplastic elastomeric (TPE) materials and their use in outdoor electrical insulation*. Rev. Adv. Mater. Sci, 2011. **29**(2011): p. 30-115.
5. AlMa'adeed, M.A.-A. and I. Krupa, *Polyolefin compounds and materials*. Springer Series on Polymer and Composite Materials, 2016: p. 271-284.
6. Dratora, P., R. Santana, and A. Moreira, *The influence of long chain branches of LLDPE on processability and physical properties*. Polímeros, 2015. **25**.
7. Zhong, X., et al., *Polyethylene plastic production process*. Insight - Material Science, 2018. **1**: p. 1.
8. Raj, B., *Plastics and their role in food packaging*. 2020.
9. *Polyethylene : General properties*. 2015; Available from: [http://www.qenos.com/internet/home.nsf/\(LUImages\)/TG1GenProp/\\$File/TG1GenProp.pdf](http://www.qenos.com/internet/home.nsf/(LUImages)/TG1GenProp/$File/TG1GenProp.pdf).
10. Petrie, E.M., *Adhesive Bonding of Polyolefin*. Polyurethane. **38**: p. 85.
11. Ozdemir, M., C.U. Yurteri, and H. Sadikoglu, *Physical polymer surface modification methods and applications in food packaging polymers*. Critical reviews in food science and nutrition, 1999. **39**(5): p. 457-477.
12. Shojaei, A., R. Fathi, and N. Sheikh, *Adhesion modification of polyethylenes for metallization using radiation-induced grafting of vinyl monomers*. Surface and Coatings Technology, 2007. **201**(16-17): p. 7519-7529.
13. Cruz, R.M.S., B.P.M. Rico, and M.C. Vieira, *9 - Food packaging and migration*, in *Food Quality and Shelf Life*, C.M. Galanakis, Editor. 2019, Academic Press. p. 281-301.
14. Engfors, M., *Commercial mobile platforms in an industrial environment*. 2011.
15. *Recyclable TetraPak cartons*. 2021; Available from: <https://www.tetrapak.com/en-in/sustainability/planet/good-for-you-good-for-the-earth/tetra-pak-cartons-recyclable>.
16. Abreu, M., *Recycling of Tetra Pak aseptic cartons*. PACKAGING INDIA, 2007. **39**(6): p. 17.
17. Walsh, H. and J. Kerry, *Packaging of ready-to-serve and retail-ready meat, poultry and seafood products*, in *Advances in meat, poultry and seafood packaging*. 2012, Elsevier. p. 406-436.
18. *Packaging material for Tetra Pak carton packages*. Available from: <https://www.tetrapak.com/en-th/solutions/packaging/packaging-material/materials>.
19. Buelens, M., et al., *What happens to used beverage cartons*. Tetra Pak Brochure, 2001. **5**.
20. Pietikäinen, V., *Collection and recycling of beverage cartons at AIT*. Project report, 2008.
21. Kasalkova, N.S., et al., *Wettability and other surface properties of modified*

- polymers. Wetting and Wettability*, 2015: p. 323-356.
22. Drnovska, H., et al., *Surface properties of polyethylene after low-temperature plasma treatment*. *Colloid and Polymer Science*, 2003. **281**(11): p. 1025-1033.
 23. Wolf, R.A., *Introduction*, in *Plastic Surface Modification*, R.A. Wolf, Editor. 2010, Hanser. p. 1-2.
 24. Gilliam, M., *Polymer Surface Treatment and Coating Technologies*, in *Handbook of Manufacturing Engineering and Technology*, A. Nee, Editor. 2013, Springer London: London. p. 1-23.
 25. Pinto, A.G., et al., *Shear strength of adhesively bonded polyolefins with minimal surface preparation*. *International Journal of Adhesion and Adhesives*, 2008. **28**(8): p. 452-456.
 26. Subedi, D.P., et al., *Surface modification of polycarbonate (bisphenol A) by low pressure rf plasma*. *Himalayan Journal of Sciences*, 2003. **1**(2): p. 115-118.
 27. Egitto, F.D. and L.J. Matienzo, *Plasma modification of polymer surfaces for adhesion improvement*. *IBM Journal of Research and Development*, 1994. **38**(4): p. 423-439.
 28. Miyamoto, K., *Plasma physics for controlled fusion*. Vol. 92. 2016: Springer.
 29. Bogaerts, A., et al., *Gas discharge plasmas and their applications*. *Spectrochimica Acta Part B: Atomic Spectroscopy*, 2002. **57**(4): p. 609-658.
 30. De Las Heras, E., et al., *Surface modification by plasma-based processes*, in *Functional Properties Of Bio-Inspired Surfaces: Characterization and Technological Applications*. 2009, World Scientific. p. 343-378.
 31. Guo, H., et al., *Non-equilibrium synergistic effects in atmospheric pressure plasmas*. *Scientific reports*, 2018. **8**(1): p. 1-10.
 32. Misra, N., O. Schlüter, and P. Cullen, *Plasma in food and agriculture*, in *Cold plasma in food and agriculture*. 2016, Elsevier. p. 1-16.
 33. Varilla, C., M. Marcone, and G.A. Annor, *Potential of Cold Plasma Technology in Ensuring the Safety of Foods and Agricultural Produce: A Review*. *Foods*, 2020. **9**(10): p. 1435.
 34. Denes, F.S. and S. Manolache, *Macromolecular plasma-chemistry: an emerging field of polymer science*. *Progress in polymer science*, 2004. **29**(8): p. 815-885.
 35. Bazaka, K., et al., *Plasma-assisted surface modification of organic biopolymers to prevent bacterial attachment*. *Acta biomaterialia*, 2011. **7**(5): p. 2015-2028.
 36. Bazaka, K., et al., *Anti-bacterial surfaces: natural agents, mechanisms of action, and plasma surface modification*. *Rsc Advances*, 2015. **5**(60): p. 48739-48759.
 37. Nikolic, V., S. Velickovic, and A. Popovic, *Biodegradation of polystyrene-graft-starch copolymers in three different types of soil*. *Environmental Science and Pollution Research*, 2014. **21**(16): p. 9877-9886.
 38. Sánchez, L.D., et al., *Surface modification of electrospun fibres for biomedical applications: A focus on radical polymerization methods*. *Biomaterials*, 2016. **106**: p. 24-45.
 39. Kim, P.-H. and S.W. Kim, *Polymer-based delivery of glucagon-like peptide-1 for the treatment of diabetes*. *International Scholarly Research Notices*, 2012. **2012**.
 40. Mohammadi Sejoubasari, R., et al., *"Grafting-through": growing polymer brushes by supplying monomers through the surface*. *Macromolecules*, 2016. **49**(7): p. 2477-2483.
 41. Pergal, M.V., et al., *In vitro biocompatibility evaluation of novel urethane-*

- siloxane co-polymers based on poly (ϵ -caprolactone)-block-poly (dimethylsiloxane)-block-poly (ϵ -caprolactone).* Journal of Biomaterials Science, Polymer Edition, 2012. **23**(13): p. 1629-1657.
42. Bhattacharya, A. and B. Misra, *Grafting: a versatile means to modify polymers: techniques, factors and applications.* Progress in polymer science, 2004. **29**(8): p. 767-814.
 43. Uyama, Y., K. Kato, and Y. Ikada, *Surface modification of polymers by grafting.* Grafting/Characterization Techniques/Kinetic Modeling, 1998: p. 1-39.
 44. Matyjaszewski, K., *Atom Transfer Radical Polymerization (ATRP): Current Status and Future Perspectives.* Macromolecules, 2012. **45**: p. 4015-4039.
 45. Gowda, D., et al., *Polymer Grafting-An Overview.* American Journal of Pharmaceutical Research, 2016. **6**: p. 2-12.
 46. Verbeek, J. and S. Hanipah, *Grafting Itaconic Anhydride onto Polyethylene Using Extrusion.* Journal of Applied Polymer Science, 2010. **116**.
 47. Malmström, J., et al., *Grafting from Poly(3,4-ethylenedioxythiophene): A Simple Route to Versatile Electrically Addressable Surfaces.* Macromolecules, 2013. **46**(12): p. 4955-4965.
 48. Maione, S., et al., *Effect of the graft ratio on the properties of polythiophene-g-poly(ethylene glycol).* Journal of Polymer Science Part B: Polymer Physics, 2015. **53**(4): p. 239-252.
 49. Hackett, A.J., et al., *Polymer-Grafted Conjugated Polymers as Functional Biointerfaces.* Conjugated Polymers for Biological and Biomedical Applications, 2018.
 50. Brogly, M., *Forces Involved in Adhesion,* in *Handbook of Adhesion Technology,* L.F.M. da Silva, A. Öchsner, and R.D. Adams, Editors. 2017, Springer International Publishing: Cham. p. 1-28.
 51. Awaja, F., et al., *Adhesion of polymers.* Progress in Polymer Science, 2009. **34**: p. 948-968.
 52. Comyn, J., *Adhesion science.* 1997: Royal Society of Chemistry London.
 53. Roesner, A., et al., *Laser Assisted Joining of Plastic Metal Hybrids.* *Phys Procedia* 12: 370–377. 2011.
 54. Ishizaka, K. and S. Lewis, *The Low Adhesion Problem due to Leaf Contamination in the Wheel/Rail Contact: Bonding and Low Adhesion Mechanisms.* *Wear*, 2017. **378**.
 55. Lipatov, I.U.r.S. and Y.S. Lipatov, *Polymer reinforcement.* 1995: ChemTec Publishing.
 56. Brewis, D. and I. Mathieson, *Adhesion and bonding to polyolefins.* Vol. 12. 2001: iSmithers Rapra Publishing.
 57. Yang, X.M., et al., *Silicon wafer wettability and aging behaviors: Impact on gold thin-film morphology.* *Materials Science in Semiconductor Processing*, 2014. **26**: p. 25–32.
 58. Pascual, M., et al., *Surface modification of low density polyethylene (LDPE) film using corona discharge plasma for technological applications.* *Journal of adhesion science and technology*, 2008. **22**(13): p. 1425-1442.
 59. Santos, L.P., J.S. Bernardes, and F. Galembeck, *Corona-treated polyethylene films are macroscopic charge bilayers.* *Langmuir*, 2013. **29**(3): p. 892-901.
 60. Amirou, S., et al., *Effects of corona discharge treatment on the mechanical properties of biocomposites from polylactic acid and Algerian date palm fibres.* *Scientific Research and Essays (SRE)*, 2013. **8**(21): p. 946-952.

61. *Chapter 17 - Adhesive Bonding*, in *Handbook of Plastics Joining (Second Edition)*, M.J. Troughton, Editor. 2009, William Andrew Publishing: Boston. p. 145-173.
62. *Chapter 3 - Material Surface Preparation Techniques*, in *Adhesives Technology Handbook (Second Edition)*, S. Ebnesajjad, Editor. 2009, William Andrew Publishing: Norwich, NY. p. 37-46.
63. Lindner, M., et al., *Surface energy of corona treated PP, PE and PET films, its alteration as function of storage time and the effect of various corona dosages on their bond strength after lamination*. Journal of Applied Polymer Science, 2018. **135**(11): p. 45842.
64. Abd El-Gelil, G.M., et al., *Degradation of Eosin Y in Water by Corona Treatment with a Dielectric Barrier Discharge Plasma*. Chemical Engineering & Technology, 2020. **43**(10): p. 2015-2022.
65. Yehia, A., *Characteristics of the dielectric barrier corona discharges*. AIP Advances, 2019. **9**(4): p. 045214.
66. Sellin, N. and J.S.d.C. Campos, *Surface composition analysis of PP films treated by corona discharge*. Materials Research, 2003. **6**(2): p. 163-166.
67. Popelka, A., et al., *Improvement of aluminum/polyethylene adhesion through corona discharge*. Journal of Physics D: Applied Physics, 2016. **50**(3): p. 035204.
68. Banerjee, S.S., et al., *Poly(ethylene glycol)-Prodrug Conjugates: Concept, Design, and Applications*. Journal of drug delivery, 2012. **2012**: p. 103973-103973.
69. Hoang Thi, T.T., et al., *The importance of poly (ethylene glycol) alternatives for overcoming PEG immunogenicity in drug delivery and bioconjugation*. Polymers, 2020. **12**(2): p. 298.
70. Zarrintaj, P., et al., *Chapter 18 - Application of compatibilized polymer blends in biomedical fields*, in *Compatibilization of Polymer Blends*, A. A.R and S. Thomas, Editors. 2020, Elsevier. p. 511-537.
71. McPherson, T.B., H.S. Shim, and K. Park, *Grafting of PEO to glass, nitinol, and pyrolytic carbon surfaces by gamma irradiation*. J Biomed Mater Res, 1997. **38**(4): p. 289-302.
72. Lakshmi, S. and A. Jayakrishnan, *Migration resistant, blood-compatible plasticized polyvinyl chloride for medical and related applications*. Artif Organs, 1998. **22**(3): p. 222-9.
73. Cheng, G., Z. Cai, and L. Wang, *Biocompatibility and biodegradation of poly(hydroxybutyrate)/poly(ethylene glycol) blend films*. J Mater Sci Mater Med, 2003. **14**(12): p. 1073-8.
74. Zacchigna, M., et al., *Multimeric, multifunctional derivatives of poly (ethylene glycol)*. Polymers, 2011. **3**(3): p. 1076-1090.
75. Sun, D., K. Iqbal, and M.O.R. Siddiqui, *20 - Thermal analysis of temperature responsive fibrous materials*, in *Thermal Analysis of Textiles and Fibers*, M. Jaffe and J.D. Menczel, Editors. 2020, Woodhead Publishing. p. 335-353.
76. Zia, F., et al., *Chapter 16 - Alginate-Poly(Ethylene) Glycol and Poly(Ethylene) Oxide Blend Materials*, in *Algae Based Polymers, Blends, and Composites*, K.M. Zia, M. Zuber, and M. Ali, Editors. 2017, Elsevier. p. 581-601.
77. Gelardi, G., et al., *9 - Chemistry of chemical admixtures*, in *Science and Technology of Concrete Admixtures*, P.-C. Aïtcin and R.J. Flatt, Editors. 2016, Woodhead Publishing. p. 149-218.
78. Chen, G., et al., *Grafting of PEG400 onto the surface of LLDPE/SMA film*.

- Frontiers of Chemical Engineering in China, 2007. **1**(2): p. 128-131.
79. Liu, L., et al., *A mild method for surface-grafting PEG onto segmented poly (ester-urethane) film with high grafting density for biomedical purpose*. *Polymers*, 2018. **10**(10): p. 1125.
 80. Ebnesajjad, S. and A.H. Landrock, *Chapter 2 - Surface Tension and Its Measurement*, in *Adhesives Technology Handbook (Third Edition)*, S. Ebnesajjad and A.H. Landrock, Editors. 2015, William Andrew Publishing: Boston. p. 19-34.
 81. Wu, S., *Polymer interface and adhesion*. 1982.
 82. Tripathi, D. and T.K. Dey, *Thermal conductivity, coefficient of linear thermal expansion and mechanical properties of LDPE/Ni composites*. *Indian Journal of Physics*, 2013. **87**(5): p. 435-445.
 83. Takke, V., et al., *Surface and adhesion properties of poly (ethylene glycol) on polyester (polyethylene terephthalate) fabric surface: Effect of air-atmospheric plasma treatment*. *Journal of Applied Polymer Science*, 2011. **122**(4): p. 2621-2629.
 84. Kumar, B.R. and T.S. Rao, *AFM studies on surface morphology, topography and texture of nanostructured zinc aluminum oxide thin films*. *Digest Journal of Nanomaterials and Biostructures*, 2012. **7**(4): p. 1881-1889.
 85. Gaff, M., M. Gašparík, and M. Kvietková, *Evaluation of wood surface quality depending on the embossing parameters*. *Wood research*, 2017. **62**: p. 751-762.
 86. Chastain, J. and R.C. King Jr, *Handbook of X-ray photoelectron spectroscopy*. Perkin-Elmer Corporation, 1992. **40**: p. 221.
 87. Riley, A., *Basics of polymer chemistry for packaging materials*, in *Packaging Technology*. 2012, Elsevier. p. 262-286.
 88. McKeen, L., *Introduction to the Physical, Mechanical, and Thermal Properties of Plastics and Elastomers*. 2018. p. 63-90.
 89. Williams, D.L. and T.M. O'Bryon, *Chapter 5 - Cleanliness Verification on Large Surfaces: Instilling Confidence in Contact Angle Techniques*, in *Developments in Surface Contamination and Cleaning*, R. Kohli and K.L. Mittal, Editors. 2013, William Andrew Publishing: Oxford. p. 163-181.
 90. Jung, M., et al., *Validation of ATR FT-IR to identify polymers of plastic marine debris, including those ingested by marine organisms*. *Marine Pollution Bulletin*, 2017. **127**.
 91. Ganji, M., et al., *DNA binding proteins explore multiple local configurations during docking via rapid rebinding*. *Nucleic acids research*, 2016. **44**(17): p. 8376-8384.